STEM CELLS
TISSUE-SPECIFIC STEM CELLS

Astrocyte Differentiation of Neural Precursor Cells is Enhanced by Retinoic Acid Through a Change in Epigenetic Modification

HIROTSUGU ASANO, MAKOTO AONUMA, TSUKASA SANOSAKA, JUN KOHYAMA, MASAKAZU NAMIHIRA, KINICHI NAKASHIMA

Laboratory of Molecular Neuroscience, Graduate School of Biological Sciences, Nara Institute of Science and Technology, Ikoma, Nara, Japan

Key Words. Retinoic acid • Neural precursor cells • STAT3 • Astrocyte • Histone acetylation

ABSTRACT

Neurons, astrocytes, and oligodendrocytes—the three major cell types that comprise the central nervous system—are generated from common multipotent neural precursor cells (NPCs). Members of the interleukin-6 family of cytokines, including leukemia inhibitory factor (LIF), induce astrocyte differentiation of NPCs by activating the transcription factor signal transducer and activator of transcription 3 (STAT3). We show here that retinoic acid (RA) facilitates LIF-induced astrocyte differentiation of NPCs. RA and LIF synergistically activate the promoter of *gfap*, which encodes the astrocytic marker glial fibrillary acidic protein, and a putative RA response element in the promoter was found to be critical for this activation. Histone H3 acetylation around the STAT-binding site in the *gfap* promoter was increased in NPCs treated with RA, allowing STAT3 to gain access to the promoter more efficiently. These results suggest that RA acts in concert with LIF to induce astrocyte differentiation of NPCs through an epigenetic mechanism that involves cross-talk between distinct signaling pathways. Stem Cells *2009;27:2744–2752*

Disclosure of potential conflicts of interest is found at the end of this article.

INTRODUCTION

Multipotent neural precursor cells (NPCs) are defined as cells that can self-renew and give rise to the three major cell types in the central nervous system (CNS): neurons, astrocytes, and oligodendrocytes. However, NPCs lack multipotentiality in early gestation, and differentiate only into neurons at mid-gestation. NPCs later acquire multipotentiality and start to differentiate into astrocytes and oligodendrocytes during late gestation [1, 2]. This sequential differentiation of NPCs appears to be temporally and spatially regulated by both cell-external cues, including cytokine signaling, and cell-internal programs such as epigenetic modification [3–6].

The interleukin (IL)-6 family of cytokines share membrane glycoprotein gp130 as a critical receptor component for activation of the downstream janus kinase (JAK)-signal transducer and activator of transcription (STAT) pathway, and have been shown to induce astrocyte differentiation of NPCs [7–9]. One member of this family, leukemia inhibitory factor (LIF), signals through its heterodimeric receptor complex, which is composed of LIF receptor (LIFR)-β and gp130. Gene knockouts of LIF, LIFRβ, gp130, and STAT3 all result in impaired astrocyte differentiation in vivo, further indicating that JAK-STAT signaling contributes to astrogliogenesis in the developing CNS [8, 10–12]. Bone morphogenetic proteins (BMPs) also contribute to the expression of astrocyte-specific genes via complex formation between the BMP-downstream transcription factor Smad1 and STATs, bridged by the transcription coactivator p300/CREB-binding protein (CBP) [13, 14].

Epigenetic modifications include both DNA methylation and histone modifications such as acetylation, methylation, phosphorylation, and ubiquitinylation [15, 16]. We have previously shown that a CpG dinucleotide within the STAT3 recognition sequence in the astrocytic marker glial fibrillary acidic protein (*gfap*) gene promoter is highly methylated in NPCs at mid-gestation, when the cells have not yet acquired the potential to differentiate into astrocytes [4]. Since STAT3 is unable to bind to the methylated cognate recognition sequence [4, 17], midgestational NPCs cannot express *gfap* even when they are stimulated by astrocyte-inducing cytokines such as LIF. As gestation proceeds, however, the STAT3-binding site becomes demethylated in NPCs, enabling the cells to express *gfap* in response to LIF stimulation. Based on these findings, we have suggested that DNA methylation is a critical cell-intrinsic determinant of astrocyte differentiation during brain development [4, 6].

Histone acetylation, mediated by transcriptional coactivators having histone acetyltransferase (HAT) activity such as p300/CBP, has been shown to correlate with gene activation [15, 16]. Conversely, gene repression is associated with histone deacetylation, which favors chromatin condensation. Transcriptional repressors, such as nuclear receptor corepressor (N-CoR) and neuron-restrictive silencer factor/repressor element-1 silencing transcription factor (NRSF/REST), have

Author contributions: H.A., J.K., M.N., K.N.: designed research; H.A., M.A., T.S.: performed research; H.A., M.N., K.N.: analyzed data; H.A., M.N., K.N.: wrote the manuscript; K.N., financial support.

Correspondence: Kinichi Nakashima, Ph.D., Laboratory of Molecular Neuroscience, Graduate School of Biological Sciences, Nara Institute of Science and Technology, 8916-5, Takayama, Ikoma, Nara 630-0192, Japan. Telephone: +81-743-72-5471; Fax: +81-743-72-5479; e-mail: kin@bs.naist.jp Received February 17, 2009; accepted for publication July 2, 2009; first published online in STEM CELLS *EXPRESS* Month 00, 2009. 1066-5099/2009/$30.00/0 doi: 10.1002/stem.176

been found in complexes with histone deacetylases (HDACs) on gene regulatory regions [18, 19].

Retinoid acid (RA) acts through RA receptors (RARs), which are members of the nuclear receptor superfamily. RARs bind, together with their heterodimeric partners the retinoid X receptors (RXRs), to RA response elements (RAREs) in the promoter regions of target. In the absence of RA ligand, RARs associate with either N-CoR or silencing mediator of retinoic acid and thyroid hormone receptors (SMRT), leading to repression of target genes by recruitment of HDACs [20–24]. When RA binds to its cognate receptor, however, HDACs are released from the RAR-RXR heterodimer and transcriptional coactivators with HAT activity are instead recruited [20–23]. In addition, it has recently been reported that many HDAC-regulated genes are also targeted by RAR [25].

Expression of RA-synthesizing and -degrading enzymes and of RARs has been shown in the developing brain [26–31]. In transgenic mice carrying a reporter gene for RA signal activation, RA signaling is shown to be indeed active in embryonic brain [31–33], and gene knockouts of RA-synthesizing and -degrading enzymes and of RARs yield impaired development of the CNS [27, 30, 34–38]. Thus, it is reasonable to hypothesize that RA signaling may be involved in the fate specification of NPCs during development. Furthermore, although RA has indeed been shown to induce neuronal differentiation of NPCs [24, 39], the extent to which it participates in differentiation into other lineages remains to be fully elucidated.

Although histone acetylation has been shown to correlates with gene activation, its precise molecular mechanisms are not fully understood. In this study, we show that RA acts synergistically with LIF to induce astrocyte differentiation of NPCs. Synergistic activation of the *gfap* promoter was virtually abolished by either deletion or mutation of a putative RARE in the promoter. We also found that RA stimulation of NPCs facilitates STAT3 binding to the *gfap* promoter, probably through the relaxation of chromatin caused by RA-induced histone acetylation around the STAT3-binding site. Furthermore, as in the case of RA stimulation, treatment with the HDAC inhibitor valproic acid (VPA) increased histone acetylation in NPCs, leading to enhanced STAT3 binding to the *gfap* promoter. Our results therefore suggest that RA-induced histone acetylation participates in astrocyte differentiation of NPCs by facilitating STAT3 binding to an astrocyte-specific gene promoter.

Materials and Methods

NPC Culture

Pregnant ICR mice were used to prepare NPCs. The experimental protocols described below were performed according to the animal experimentation guidelines of Nara Institute of Science and Technology. NPCs were prepared from telencephalons of E14.5 mice and cultured as described previously [4, 13]. Briefly, the telencephalons were triturated in Hank's balanced salt solution (HBSS) by mild pipetting with a 1-ml pipet tip. Dissociated cells were cultured for 4 days in N2-supplemented Dulbecco's modified Eagle's medium (DMEM) with F12 containing 10 ng/ml basic FGF (N2/DMEM/F12/bFGF; R&D Systems Inc., Minneapolis, http://www.rndsystems.com) on culture dishes which had been precoated with poly-L-ornithine and fibronectin (Sigma-Aldrich, St. Louis, http://www.sigmaaldrich.com). Cells were detached in HBSS and replated onto chamber slides, 60-mm culture dishes, or 12-well plates (Nunc, Rochester, NY, http://www.nuncbrand.com), precoated as above, and cultured in N2/DMEM/F12/bFGF. RA (1 μM, Sigma), LIF (50 ng/ml, Chemicon, Temecula, CA, http://www.chemicon.com) and VPA (1 mM, Sigma) were added singly or in combination, as appropriate, to examine their effects on differentiation of NPCs. Cells cultured on coated chamber slides were washed with PBS, fixed in 4% paraformaldehyde in PBS, and stained with anti-GFAP antibody (DAKO, Glostrup, Denmark, http://www.dako.com) and Cy3-conjugated second antibody (Jackson Immunoresearch Laboratories, West Grove, PA, http://www.jacksonimmuno.com). Nuclei were stained using bisbenzimide H33258 fluorochrome trihydrochloride (Nacalai Tesque, Kyoto, Japan, www.nacalai.co.jp/en). Stained cells were visualized with fluorescence microscope (Axiovert 200M, Carl Zeiss, Jena, Germany, http://www.zeiss.com).

Reverse-Transcription Polymerase Chain Reaction

Total RNA was isolated from NPCs that had been cultured with LIF for 8 hours in the presence or absence of RA. Reverse transcription was performed with SuperScript II reverse transcriptase (Invitrogen, Carlsbad, CA, http://www.invitrogen.com) and polymerase chain reaction (PCR) reactions were performed using Amplitaq Gold (Applied BioSystems, Foster City, CA, http://www.appliedbiosystems.com). The following primers were used: *gfap*; GFAP-S, 5′-CACGAACGAGTCCCTAGAGC-3′. and GFAP-AS, 5′-TCACATCACCACGTCCTTG-3′; *g3pdh*; G3PDH-S, 5′- ACCACAGTCCATGCCATCAC-3′, and G3PDH-AS, 5′-TCCACCACCCTGTTGCTGT A-3′.

Promoter Assay

NPCs cultured for 4 days on 10-cm dishes as described above were replated onto 12-well plates (Nunc) and transfected the next day with a plasmid containing the firefly luciferase gene under the regulation of the 2.5-kb *gfap* promoter (GF1L) [13], the 1.9-kb *gfap* promoter (GF1LB, Fig. 3A) [13], or with a modified construct in which nucleotide substitutions were introduced into the GF1L sequences 5′-TTCCGAGAA-3′, a STAT3-binding site (GF1L-SBSPM) [4], or 5′-AGTTCAAGGTCA-3′, a putative RARE (GF1L-REPM, Fig. 3B). As an internal control, the sea pansy luciferase gene conjugated with human elongation factor-1α promoter (R-Luc) was also cotransfected [13]. Transfection was performed using Trans-IT LT1 (Mirus Bio, Madison, WI, www.mirusbio.com) according to the manufacturer's procedures. On the day after transfection, cells were stimulated with LIF (50 ng/ml) and/or RA (1 μM) for 8 hours and then solubilized. Luciferase activity was measured according to the procedures recommended for the Dual Luciferase Reporter Assay System (Promega, Madison, WI, http://www.promega.com), using Wallac 1,420 ARVO/Light (PerkinElmer Life and Analytical Sciences, Boston, MA, http://www.perkinelmer.com) luminometer was used for detection. Firefly luciferase activity was divided by sea pansy luciferase activity from the cotransfected control plasmid, R-Luc.

Chromatin Immunoprecipitation Assay

Chromatin immunoprecipitation was performed according to a protocol published by Upstate Biotechnology (Charlottesville, VA, http://www.upstate.com), with minor modifications. Cells were exposed to formaldehyde at a final concentration of 1%, added directly to the tissue culture medium. The cells were centrifuged to a pellet after 10 min of formaldehyde exposure, lysed in lysis buffer (1% SDS, 10 mM EDTA, 50 mM Tris-HCl [pH 8.1]) containing a protease inhibitor cocktail (Nacalai Tesque), and then incubated for 10 min on ice. Cell lysates were sonicated using a microtip (Branson Ultrasonics, Danbury, CT, www.bransonultrasonics.com) until the DNA fragments were 500–1,000 base pairs in length. These chromatin samples were diluted 1:10 with dilution buffer (1.1% Triton X-100, 0.11% NaDOC, 50 mM Tris-HCl [pH 8.1], 167 mM NaCl), and 2.5% of the total volume was stored as input at −20°C until use. Immunoprecipitation was performed at 4°C overnight with 2 μg of an antibody against STAT3, RARα, RARβ, RXR (Santa Cruz Biotechnology Inc., Santa Cruz, CA, http://www.scbt.com) or acetylated histone H3 (Upstate Biotechnology) after the samples were precleared with salmon sperm DNA/protein A agarose (Upstate Biotechnology).

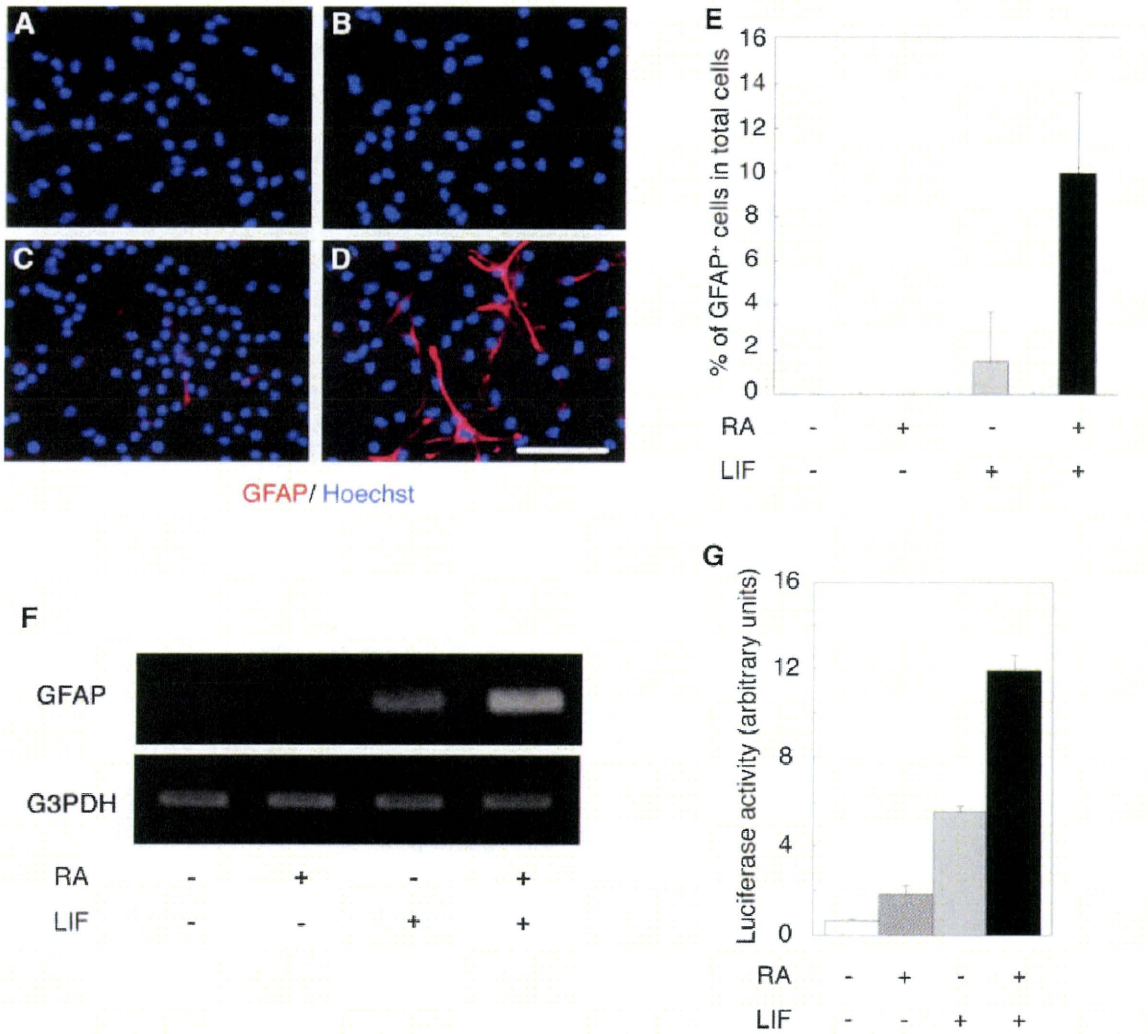

Figure 1. Synergistic induction of astrocyte differentiation of neural precursor cells (NPCs) by retinoic acid (RA) and leukemia inhibitory factor (LIF). NPCs were cultured with medium alone (**A**), RA (1 μM) (**B**), LIF (50 ng/ml) (**C**), or RA (1 μM) plus LIF (50 ng/ml) (**D**) for 2 days. The cells were then stained with antibody against glial fibrillary acidic protein (GFAP; red) and with Hoechst 33258 (blue). Scale bar = 50 μm. (**E**): Percentage of GFAP-positive cells in total cells was calculated. (**F**): Total RNA was extracted from NPCs cultured as above with medium alone, RA, LIF, or RA plus LIF, and was analyzed by reverse-transcription polymerase chain reaction using specific primers for *gfap* and *g3pdh*. (**G**): *gfap* promoter assays were performed for cells transfected with a firefly luciferase gene reporter construct containing the 2.5-kb mouse *gfap* promoter (GF1L) along with R-Luc, following incubation with or without RA and/or LIF for 8 hours. Data in graphs are mean ± SD.

Immune complexes were collected by salmon sperm DNA/protein A agarose and washed successively with the following buffers: low-salt buffer (0.1% SDS, 1% Triton X-100, 0.1% NaDOC, 1 mM EDTA, 50 mM Tris-HCl [pH 8.1], 167 mM NaCl), high-salt buffer (0.1% SDS, 1% Triton X-100, 0.1% NaDOC, 1 mM EDTA, 50 mM Tris-HCl [pH 8.1], 500 mM NaCl), LiCl buffer (0.25 M LiCl, 0.5% NP-40, 0.5% NaDOC, 1 mM EDTA, 10 mM Tris-HCl [pH 8.1]), and TE buffer (10 mM Tris-HCl, 1 mM EDTA [pH 8.0]). Immune complexes were disrupted with direct elution buffer (0.5% SDS, 5 mM EDTA, 10 mM Tris-HCl [pH 8.1], 300 mM NaCl) and the covalent links between immunoprecipitates and input chromatin were disrupted by incubation with 300 mM NaCl at 65°C for 4 hours or overnight. DNA was further incubated with RNase and proteinase K (Nacalai Tesque), purified by phenol extraction, and ethanol precipitated. DNA pellets were dissolved in 20 μl of H_2O and used as a template for PCR or quantitative PCR (qPCR). The following sets of primers were used: GSS (5′-TAAGCTGAAGACCTGGCAGTG-3′) and GSAS (5′-TGCTGAATAGAGCCTTGTTCTC-3′) for PCR, GSSQ (5′-TGACTCACCTTGGCATAGACAT-3′) and GSASQ (5′-CTGCTTTTATCCCAGGATGC-3′) for qPCR of the STAT3-binding site-containing region of the *gfap* promoter, GF-RARE-S (5′-CACAGGAGGTGTGGTGGCTA-3′) and GF-RARE-AS (5′-GGTTTGTCAGCAACGCTGGA-3′) for PCR, GF-RARE-SQ (5′-GCTTAAGGCTGGAAGACACAG -3′) and GF-RARE-ASQ, (5′-CTGGATCTAGGACTTGCTTCGT-3′) for qPCR of the RARE-containing region of the *gfap* promoter.

Results

RA and LIF Synergistically Induce Astrocyte Differentiation of NPCs

As a first step toward testing the possibility that RA signaling plays a role in fate specification of NPCs, we examined the

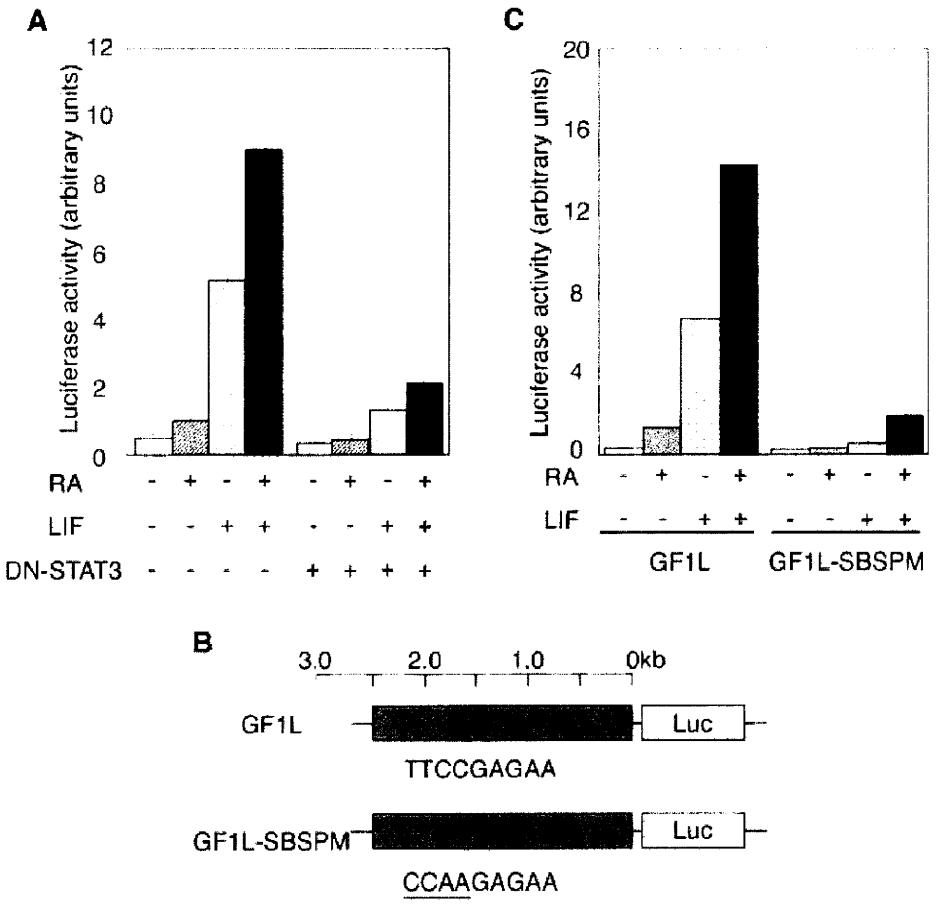

Figure 2. STAT3 is required for the synergy between retinoic acid (RA) and leukemia inhibitory factor (LIF). **(A):** Neural precursor cells (NPCs) were transfected with an expression plasmid encoding $STAT3^{Y705F}$ (DN-STAT3) or a control vector together with GF1L along with R-Luc. The cells were incubated with or without RA (1 μM) and LIF (50 ng/ml) for 8 hours. **(B):** NPCs were transfected either with GF1L or with GF1L-SBSPM (mutated in the STAT3 recognition sequence), along with R-Luc, and incubated with or without RA (1 μM) and LIF (50 ng/ml) for 8 hours. Data are mean ± SD.

expression of RAR and RXR family genes in NPCs and found that they were indeed expressed (supporting information Fig. 1). We next investigated the effect of RA on astrocyte differentiation of NPCs. NPCs prepared from E14.5 mouse telencephalons were cultured for 2 days with RA, with LIF, with RA together with LIF, or left untreated. The cells were then stained with an antibody against the astrocyte-specific marker GFAP. As shown in Figure 1, a small number of GFAP-positive astrocytes were induced in the presence of LIF, whereas RA alone induced no GFAP-positive cells (Fig. 1A–C, 1E). However, GFAP-positive astrocyte differentiation was induced synergistically when the NPCs were treated simultaneously with RA and LIF (Fig. 1D, 1E). We also examined another astrocytic marker, S100β, whose expression begins earlier than that of GFAP in the course of astrocytic differentiation [40]. In contrast to the case of GFAP, RA alone induced S100β–positive cells in NPCs (supporting information Fig. 2). This is probably because that S100β is an earlier marker for astrocyte differentiation than GFAP [40]. Therefore, this gene has already become competent to be induced by either RA or LIF alone by this developmental stage, although the precise mechanism is currently unknown.

To unravel the mechanism whereby RA and LIF synergistically induce GFAP-positive astrocyte differentiation of NPCs, we next performed RT-PCR analysis. *gfap* mRNA increased markedly in the costimulated condition with RA and LIF compared to treatments with LIF or RA alone (Fig. 1F), indicating that RA acts at the transcriptional level to enhance LIF-induced GFAP-positive astrocyte differentiation.

Given that RA affects *gfap* expression, we carried out a reporter assay using the *gfap* promoter construct GF1L-pGL3 [4, 13]. As shown in Figure 1G, although the *gfap* promoter was barely activated by RA alone, synergistic activation was observed when the NPCs were treated with RA and LIF simultaneously. These results indicate that RA and LIF synergistically induce astrocyte differentiation of NPCs.

STAT3 Is Essential for Synergistic Activation of the *Gfap* Promoter by RA and LIF

STAT3 plays a critical role as a downstream molecule in IL-6 family cytokine-signaling pathways [4, 7, 8, 13]. Therefore, to investigate whether STAT3 is also essential for synergistic activation of the *gfap* promoter by RA and LIF, we performed

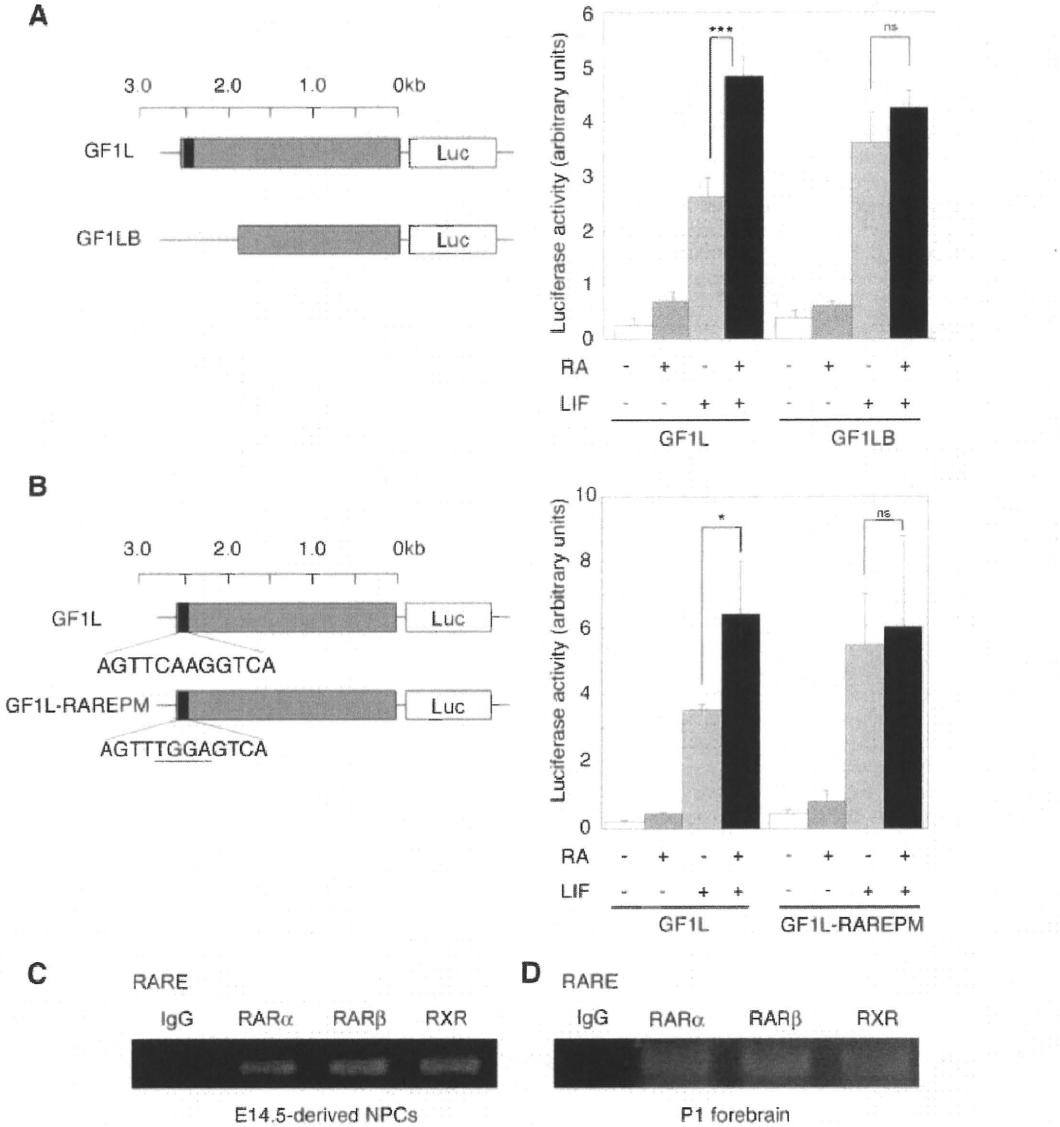

Figure 3. A retinoic acid response element (RARE) in the *gfap* promoter is essential for the synergistic activation by retinoic acid (RA) and leukemia inhibitory factor (LIF). Neural precursor cells (NPCs) were transfected with either GF1L or GF1LB (**A**), or GF1L-RAREPM (**B**), along with R-Luc, and incubated with or without RA (1 μM) for 8 hours. Data are mean ± SD. Statistical significance was examined by the Student's *t*-test. *, $p < .05$; ***, $p < .005$; NS, not significant ($p = .143$ in **A**, $p = .248$ in **B**). Chromatin immunoprecipitation assays for E14.5 forebrain-derived NPCs (**C**) and freshly prepared P1 forebrain (**D**) were performed using anti-RARα, RARβ, RXR, and control IgG antibody, and followed by polymerase chain reaction with primers targeted to a fragment including the RARE in the *gfap* promoter.

a reporter assay using GF1L-pGL3 in combination with a construct expressing a dominant-negative form of STAT3 (DN-STAT3) in which tyrosine 705 of STAT3 is substituted by phenylalanine [13]. As expected, expression of DN-STAT3 in NPCs suppressed the activation of the *gfap* promoter by LIF (Fig. 2A). Furthermore, DN-STAT3 dramatically inhibited the activation of the promoter induced by simultaneous addition of RA and LIF. We have previously shown that a STAT-binding site (TTCCGAGAA) located 1.5 kb upstream of the *gfap* transcription initiation site is indispensable for STAT3 to activate the *gfap* promoter. When this site was mutated to *CCAA*GAGAA (Fig. 2B), activation of the *gfap* promoter by combined treatment with RA and LIF, as well as with LIF alone, was virtually abolished (Fig. 2B). Collectively, these results reveal that the activation of STAT3 and its binding to the cognate recognition site are essential for the synergistic activation of the *gfap* promoter induced by RA and LIF.

A RARE in the *Gfap* Promoter Is Critical for Synergistic Activation Induced by RA and LIF

We identified a putative RARE site (AGTTCAAGGTCA) located 2.5 kb upstream of the *gfap* transcription start site. To determine whether this RARE is important for the synergistic activation of the promoter by RA and LIF, we next tested the

responsiveness of the deleted *gfap* promoter construct GF1LB, which lacks a 0.6-kb fragment that spans the RARE (Fig. 3A) [13]. It has been shown that, in the absence of ligands, the RAR/RXR heterodimer functions as a transcriptional suppressor by forming a complex with corepressor molecules such as N-CoR and SMRT [20, 24, 41, 42]. Consistent with these findings, the responsiveness of GF1LB to LIF stimulation was augmented relative to GF1L, probably due to deletion of the region containing the RARE. There was no further augmentation of LIF-induced activation of GF1LB by RA stimulation (Fig. 3A). We also obtained similar results to those with the deletion construct when nucleotide substitutions were made in the RARE (AGTT*TGGA*GTCA, GF1L-RAREPM) (Fig. 3B).

We next examined whether RAR/RXR indeed associates with the region of the *gfap* promoter containing the RARE, by chromatin immunoprecipitation (ChIP) assay using specific antibodies against RARα, RARβ, and RXR. As shown in Figure 3C and D, binding of RARα, RARβ, and RXR to the RARE-containing region was detected in cultured NPCs and in the forebrain at postnatal day 1 (P1) when astrocytogenesis is intensively occurring [2, 43]. These results suggest that the RARE in the *gfap* promoter plays a critical role in the synergistic action of RA and LIF.

We then sought to examine whether RA signaling is in fact activated in the P1 brain in vivo. To this end, we introduced luciferase construct containing 3× RARE (pGL3-RARE) to P1 forebrain by electroporation with or without a plasmid expressing dominant negative form of RARα (RAR403) in which transcriptional activation domain is deleted [44]. On the following day, dissociated cells from the forebrain were subjected to a reporter assay. As shown in supporting information Figure 3, we observed an activation of the reporter and this activation was completely inhibited by the expression of RAR403, suggesting that RA signaling is actually activated in vivo during astrocytogenesis.

RA Increases Histone H3 Acetylation Around the STAT-binding Site in the *gfap* Promoter, Thus Enhancing STAT3 Binding to the Promoter

Upon binding of RA to RAR/RXR, the transcriptional repressor complex has been shown to be replaced by coactivator molecules, including p300/CBP, that possess histone acetyltransferase activity [20, 41, 42]. In support of this, we confirmed RA-induced exchange of association factor with RARα by a coimmunoprecipitation assay in the presence or absence of RA in 293T cells transfected with Myc-RARα, N-CoR-FLAG, and p300-HA expressing constructs (supporting information Fig. 4). Since histone acetylation is considered to relax chromatin structure, allowing gene transcription [16, 45], we hypothesized that the mechanism of synergistic action of RA and LIF on the *gfap* promoter might involve an alteration of histone acetylation. To test this hypothesis, we carried out a ChIP assay, using a specific antibody for acetylated histone H3, in NPCs stimulated with RA. As shown in Figure 4B, histone H3 acetylation was enhanced not only in the RARE-containing region but also in the STAT site-containing region of the *gfap* promoter in response to RA; this increased acetylation may enable STAT3 to bind more efficiently to the relaxed promoter. Moreover, we observed an enhancement of LIF-induced STAT3 binding to the *gfap* promoter when the cells were costimulated with RA (Fig. 4C). Thus, these results suggest that RA facilitates STAT3 binding to the promoter through an alteration in chromatin modification.

Since it has been shown that there was an inverse correlation between DNA methylation status of the *gfap* promoter

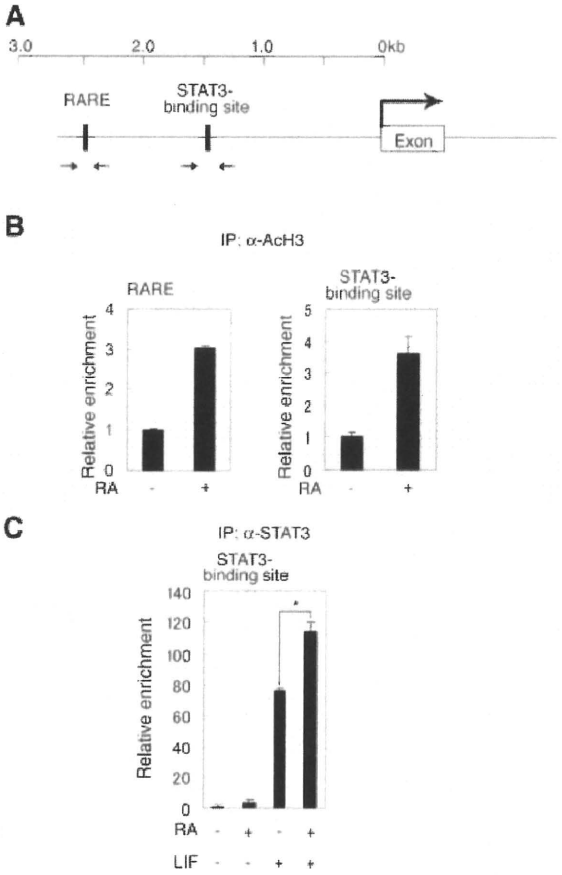

Figure 4. Retinoic acid (RA)-induced histone H3 acetylation in the STAT site-containing region facilitates STAT3 binding to the *gfap* promoter. (**A**): Schematic diagram of the *gfap* promoter showing the locations of the retinoic acid response element (RARE) and STAT3-binding sequences. Arrows indicate the locations of primers used in qPCR for chromatin immunoprecipitation (ChIP) assays in (**B**) or (**C**). Cells were stimulated with or without RA (1 μM) and leukemia inhibitory factor (50 ng/ml) for 20 minutes. ChIP assays were performed using antiacetylated histone H3 and IgG antibodies (**B**), or anti-STAT3 and IgG antibodies (**C**), followed by polymerase chain reaction with primers targeted to fragments including the RARE or STAT3-binding site in the *gfap* promoter as indicated. Data are mean ± SD. Statistical significance was examined by the Student's *t*-test. *, $p < .05$.

containing STAT3 binding site and the potential of cells to express *gfap* [4, 46, 47], we next examined whether methylation of the promoter region was affected by RA stimulation using bisulfite sequence method. However, in agreement with previous reports [4, 46, 47], almost all CpG sites at *gfap* promoter had become almost demethylated in 4-day-cultured NPCs, and this was not further changed even after additional 2-day culture with RA (data not shown).

Histone Acetylation Promoted by HDAC Inhibition Mimics the Effect of RA on Astrocytic Differentiation of NPCs

To further explore the relationship between histone acetylation and astrocytic differentiation of NPCs, we sought to determine whether treatment with the HDAC inhibitor valproic acid (VPA; 2-propylpentanoic acid) [48] affects GFAP-positive astrocyte differentiation of NPCs. Although VPA

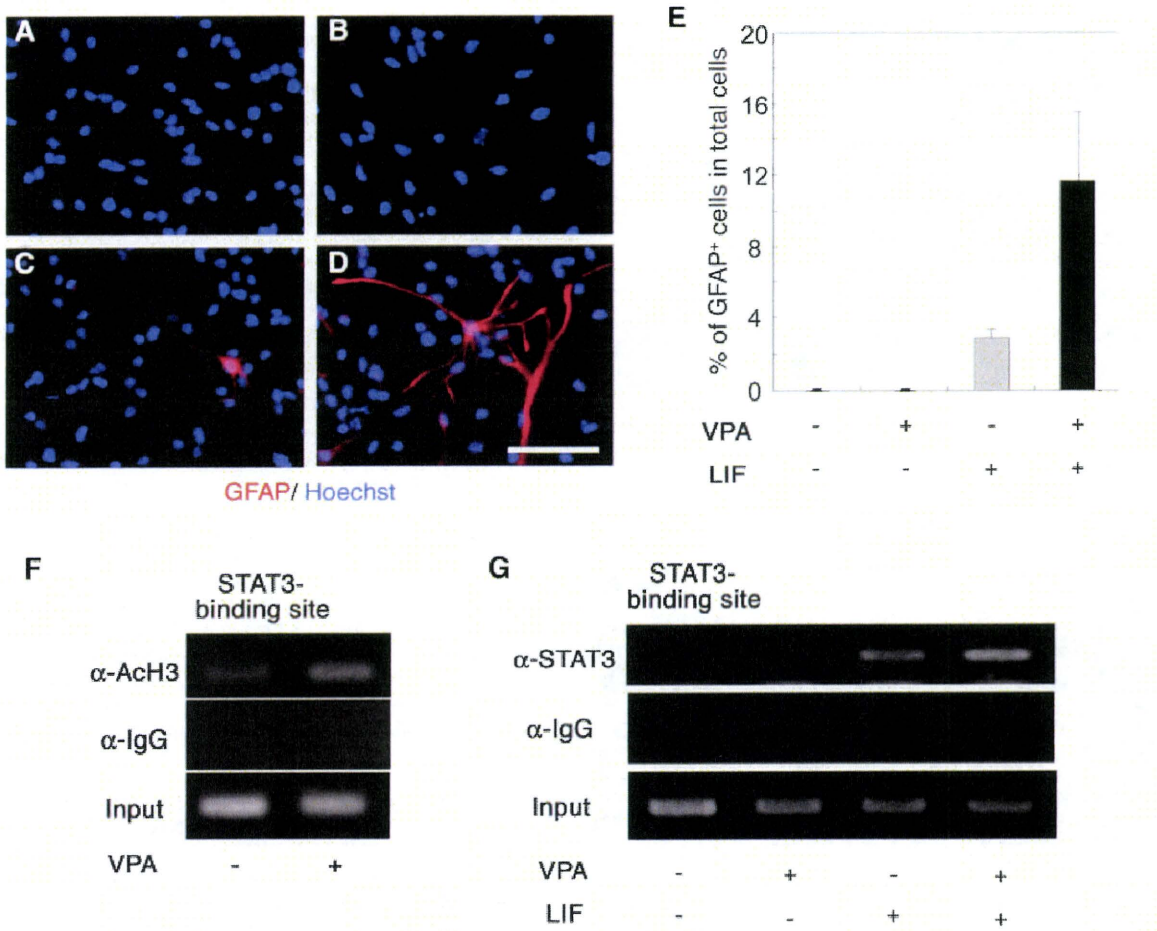

Figure 5. The histone deacetylases inhibitor valproic acid (VPA) promotes leukemia inhibitory factor (LIF)-induced astrocyte differentiation of neural precursor cells. Cells were cultured with medium alone (**A**), VPA (1 mM) (**B**), LIF (50 ng/ml) (**C**), or VPA (1 mM) plus LIF (50 ng/ml) (**D**) for 2 days, and then stained with an antibody against glial fibrillary acidic protein (GFAP; red) and with Hoechst 33258 (blue). Scale bar = 50 μm. (**E**): Percentage of GFAP-positive cells in total cells was calculated. Data are mean ± SD. Chromatin immunoprecipitation assays were performed using anti-acetylated histone H3 and IgG antibodies (**F**), or anti-STAT3 and IgG antibodies (**G**), and followed by polymerase chain reaction with primers targeted to a fragment including the STAT3-binding sequence within the *gfap* promoter.

itself did not induce GFAP-positive cells, we observed that VPA and LIF synergistically induced GFAP-positive astrocyte differentiation of NPCs (Fig. 5A–E), as in the case of RA and LIF. We further confirmed that histone H3 acetylation around the STAT3-binding site was increased by VPA treatment in NPCs (Fig. 5F). Finally, we tested the association of STAT3 with the *gfap* promoter by ChIP assay, and found that STAT3 bound more effectively to the promoter in the presence of both VPA and LIF than with LIF alone (Fig. 5G). Taken together, these results suggest that histone acetylation enhances STAT3 binding to the *gfap* promoter and thereby plays an important role in astrocyte differentiation of NPCs that have been synergistically induced by RA and LIF.

Discussion

It was reported recently that, at relatively late gestation, RA promotes astrocyte differentiation of NPCs induced by ciliary neurotrophic factor (CNTF), a member of the IL-6 cytokine family that activates the same gp130-JAK-STAT pathway as does LIF [49]. However, a mechanism to explain this function of RA has yet to be presented. In this study, we have shown that RA synergistically induces astrocyte differentiation of NPCs in cooperation with LIF, a plausible explanation for which is that RA enhances histone H3 acetylation around the STAT3-binding site in the *gfap* promoter, thus making the site more accessible to STAT3 (Fig. 6). Moreover, we found that histone acetylation induced by VPA also promoted LIF-induced astrocyte differentiation. Taken together, these results indicate that RA-induced alteration of histone acetylation regulates astrocyte differentiation of NPCs by facilitating STAT3 binding to the astrocyte-specific gene promoter. In this context, O'Donnell et al. [50] have recently shown that histone acetylation induced by the ETS domain transcription factor ELK-1 stimulates recruitment of nuclear factor IA to the *c-fos* gene promoter. Taking their and our findings into consideration, this type of mechanism (i.e., primary effectors trigger a HAT relay switch, which facilitates the recruitment of additional transcription factors) may be widespread in histone acetylation-associated gene activation.

We further found that RARα, RARβ, and RXR associate with a RARE-containing region of the *gfap* promoter, and

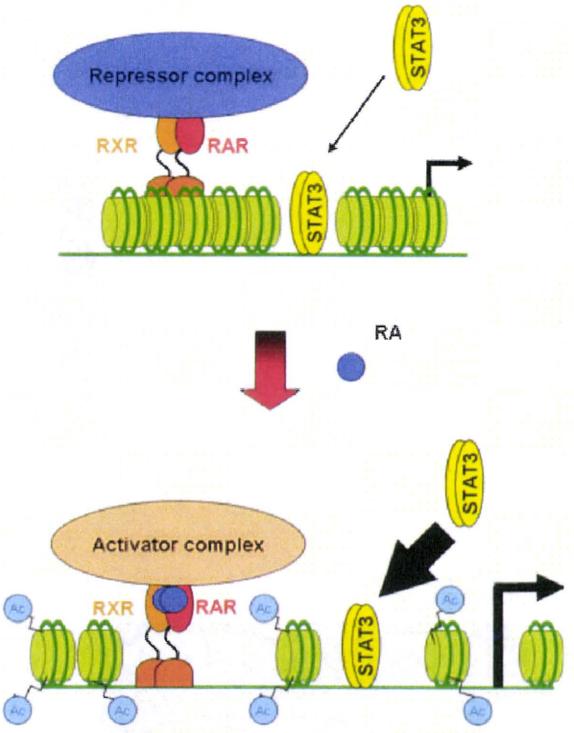

Figure 6. A model for synergistic activation of the *gfap* promoter by retinoic acid (RA) and leukemia inhibitory factor (LIF). In the absence of RA, RAR/RXR complexes with transcriptional repressors, leading to a closed chromatin structure. Upon ligand (RA) binding, the repressor complex is replaced by an activator complex, inducing a relaxed chromatin structure through histone H3 acetylation. This acetylation facilitates LIF-induced binding of STAT to its cognate sequence (see text for details). Abbreviation: Ac, acetyl group.

that either deleting this region or introducing nucleotide substitutions into the RARE augmented its responsiveness in NPCs treated with LIF alone. This is probably due to the impairment of binding of RAR/RXR, which can recruit a transcriptional repressor complex in the absence of ligand to the promoter [20–23]. It has been shown that ligand-free RAR/RXR heterodimers associate with corepressor molecules, such as N-CoR and SMRT (supporting information Fig. 4) [20–24]. A recent study indicated that astrocyte differentiation of NPCs was precociously and robustly enhanced in N-CoR-deficient embryonic forebrain, and that N-CoR-deficient NPCs did not self-renew but instead differentiated into astrocytes in vitro [18]. Moreover, overexpression of N-CoR in NPCs inhibited CNTF-mediated astrocytic differentiation. Collectively, these findings suggested that repressor complexes comprising ligand-free RAR/RXR and N-CoR are involved in the regulation of astrocyte-specific gene expression in NPCs.

It has been reported that RARα interacts with the src homology two (SH2) domain of STAT3 and that RAR/RXR associates with coactivator complexes including p300/CBP upon ligand binding [51]. In addition, STAT3 itself has been shown to associate with p300/CBP [13, 14]. It may therefore be possible that a large activator complex that includes RAR/RXR and STAT3 assembles on the *gfap* promoter in NPCs in response to combined treatment with RA and LIF. However, further experiments need to be conducted to assess this possibility.

Although gene knockouts of RAR and RA-synthesizing and -degrading enzymes, as well as the absence of retinoid in vitamin A-deficient mice, lead to defects in brain development such as abnormal positioning of the anterior and dorsal boundaries [27, 30, 34–38], the fate specification of embryonic NPCs in these mice has yet to be specifically addressed. Since we have shown here that RA promotes astrocyte differentiation of NPCs in collaboration with LIF, it will be intriguing to examine spatiotemporally regulated astrocyte differentiation of NPCs in such RA signal-dysregulated mice.

In conclusion, astrocyte differentiation of NPCs in the developing brain seems to be regulated by the intricate coordination of 1) the JAK-STAT pathway, which involves cross-talk with other signaling pathways at various steps such as regulation of STAT activation by LIF [7–9], 2) complex formation with other transcription factors [13], and 3) DNA [4] and histone modifications [50, 52, and this study].

Acknowledgments

We thank Dr. Y. Bessho and Dr. T. Matsui for valuable discussions; Dr. I. Smith and B. Juliandi for helpful comments and critical reading of the manuscript; N. Ueda and M. Tano for excellent secretarial assistance; and N. Namihira for technical help. This work was supported by the Brain Science Foundation, a Grant-in-Aid for Young Scientists, a Grant-in-Aid for Scientific Research on Priority Areas–Molecular Brain Science, and the Nara Institute of Science and Technology (NAIST) Global Center of Excellence (COE) Program from the Ministry of Education, Culture, Sports, Science and Technology of Japan.

Disclosure of Potential Conflicts of Interest

The authors indicate no potential conflicts of interest.

References

1 Qian X, Shen Q, Goderie SK et al. Timing of CNS cell generation: a programmed sequence of neuron and glial cell production from isolated murine cortical stem cells. Neuron 2000;28:69–80.
2 Sauvageot CM, Stiles CD. Molecular mechanisms controlling cortical gliogenesis. Curr Opin Neurobiol 2002;12:355–249.
3 Miller FD, Gauthier AS. Timing is everything: making neurons versus glia in the developing cortex. Neuron 2007;54:357–369.
4 Takizawa T, Nakashima K, Namihira M et al. DNA methylation is a critical cell-intrinsic determinant of astrocyte differentiation in the fetal brain. Dev Cell 2001;1:749–758.
5 Hsieh J, Gage FH. Epigenetic control of neural stem cell fate. Curr Opin Genet Dev 2004;14:461–469.
6 Namihira M, Kohyama J, Abematsu M et al. Epigenetic mechanisms regulating fate specification of neural stem cells. Philos Trans R Soc Lond B Bio Sci 2008;363:2099–2109.
7 Bonni A, Sun Y, Nadal-Vicens M et al. Regulation of gliogenesis in the central nervous system by the JAK-STAT signaling pathway. Science 1997;278:477–483.
8 Nakashima K, Wiese S, Yanagisawa M et al. Developmental requirement of gp130 signaling in neuronal survival and astrocyte differentiation. J Neurosci 1999;19:5429–5434.
9 Nakashima K, Taga T,Mechanisms underlying cytokine-mediated cell-fate regulation in the nervous system. Mol Neurobiol 2002;25:233–244.

10 Bugga L, Gadient RA, Kwan K et al. Analysis of neuronal and glial phenotypes in brains of mice deficient in leukemia inhibitory factor. J Neurobiol 1998;36:509–524.
11 Koblar SA, Turnley AM, Classon BJ et al. Neural precursor differentiation into astrocytes requires signaling through the leukemia inhibitory factor receptor. Proc Natl Acad Sci U S A 1998;95:3178–3181.
12 He F, Ge W, Martinowich K et al. A positive autoregulatory loop of Jak-STAT signaling controls the onset of astrogliogenesis. Nat Neurosci 2005;8:616–625.
13 Nakashima K, Yanagisawa M, Arakawa H et al. Synergistic signaling in fetal brain by STAT3-Smad1 complex bridged by p300. Science 1999;284:479–482.
14 Sun Y, Nadal-Vicens M, Misono S et al. Neurogenin promotes neurogenesis and inhibits glial differentiation by independent mechanisms. Cell 2001;104:365–376.
15 Jaenisch R, Bird A. Epigenetic regulation of gene expression: how the genome integrates intrinsic and environmental signals. Nat Genet 2003;33:245–254.
16 Li B, Carey M, Workman JL. The role of chromatin during transcription. Cell 2007;128:707–719.
17 Fan G, Martinowich K, Chin MH et al. DNA methylation controls the timing of astrogliogenesis through regulation of JAK-STAT signaling. Development 2005;132:3345–3356.
18 Hermanson O, Jepsen K, Rosenfeld MG. N-CoR controls differentiation of neural stem cells into astrocytes. Nature 2002;419:934–939.
19 Ballas N, Mandel G. The many faces of REST oversee epigenetic programming of neuronal genes. Curr Opin Neurobiol 2005;15:500–506.
20 Freedman LP. Increasing the complexity of coactivation in nuclear receptor signaling. Cell 1999;97:5–8.
21 Aranda A, Pascual A. Nuclear hormone receptors and gene expression. Physiol Rev 2001;81:1269–1304.
22 Gronemeyer H, Gustafsson JA, Laudet V. Principles for modulation of the nuclear receptor superfamily. Nat Rev Drug Discov 2004;3:950–964.
23 Bastien J, Rochette-Egly C. Nuclear retinoid receptors and the transcription of retinoid-target genes. Gene 2004;328:1–16.
24 Jepsen K, Solum D, Zhou T et al. SMRT-mediated repression of an H3K27 demethylase in progression from neural stem cell to neuron. Nature 2007;450:415–420.
25 Epping ME, Wang L, Plumb JA et al. A functional genetic screen identities retinoic acid signalling as a target of histone deacetylase inhibitors. Proc Natl Acad Sci U S A 2007;104:17777–17782.
26 Mollard R, Viville S, Ward SJ et al. Tissue-specific expression of retinoic acid receptor isoform transcripts in the mouse embryo. Mech Dev 2000;94:223–232.
27 Sakai Y, Meno C, Fujii H et al. The retinoic acid-inactivating enzyme CYP26 is essential for establishing an uneven distribution of retinoic acid along the anterio-posterior axis within the mouse embryo. Genes Dev 2001;15:213–225.
28 Niederreither K, McCaffery P, Drager UC et al. Restricted expression and retinoic acid-induced downregulation of the retinaldehyde dehydrogenase type 2 (RALDH-2) gene during mouse development. Mech Dev 1997;62:67–78.
29 Koide T, Downes M, Chandraratna RA et al. Active repression of RAR signaling is required for head formation. Genes Dev 2001;15:2111–2121.
30 Sirbu IO, Gresh L, Barra J et al. Shifting boundaries of retinoic acid activity control hindbrain segmental gene expression. Development 2005;132:2611–2622.
31 Rawson NE, LaMantia AS. A speculative essay on retinoic acid regulation of neural stem cells in the developing and aging olfactory system. Exp Gerontol 2007;42:46–53.
32 Rossant J, Zirngibl R, Cado D et al. Expression of a retinoic acid response element-hsplacZ transgene defines specific domains of transcriptional activity during mouse embryogenesis. Genes Dev 1991;5:1333–1344.
33 Haskell GT, Lamantia AS. Retinoic acid signaling identifies a distinct precursor population in the developing and adult forebrain. J Neurosci 2005;25:7636–7647.
34 Halilagic A, Ribes V, Ghyselinck NB et al. Retinoids control anterior and dorsal properties in the developing forebrain. Dev Biol 2007;303:362–375.
35 Dupé V, Ghyselinck NB, Wendling O et al. Key roles of retinoic acid receptors alpha and beta in the patterning of the caudal hindbrain, pharyngeal arches and otocyst in the mouse. Development 1999;126:5051–5059.
36 Wendling O, Ghyselinck NB, Chambon P et al. Roles of retinoic acid receptors in early embryonic morphogenesis and hindbrain patterning. Development 2001;128:2031–2038.
37 Ribes V, Wang Z, Dollé P et al. Retinaldehyde dehydrogenase 2 (RALDH2)-mediated retinoic acid synthesis regulates early mouse embryonic forebrain development by controlling FGF and sonic hedgehog signaling. Development 2006;133:351–361.
38 White JC, Shankar VN, Highland M et al. Defects in embryonic hindbrain development and fetal resorption resulting from vitamin A deficiency in the rat are prevented by feeding pharmacological levels of all-*trans*-retinoic acid. Proc Natl Acad Sci U S A 1998;95:13459–13464.
39 Takahashi J, Palmer TD, Gage FH. Retinoic Acid and Neurotrophins collaborate to regulate neurogenesis in adult-derived neural stem cell cultures. J Neurobiol 1999;38:65–81.
40 Burette A, Jalenques I, Romand R. Developmental distribution of astrocytic proteins in the rat cochlear nucleus. Brain Res Dev Brain Res 1998;107:179–189.
41 Xu L, Glass CK, Rosenfeld MG. Coactivator and corepressor complex in nuclear receptor function. Curr Opin Genet Dev 1999;9:140–147.
42 Perissi V, Staszewski LM, McInerney EM et al. Molecular determinants of nuclear receptor-corepressor interaction. Genes Dev 1999;13:3198–3208.
43 Parnavelas JG. Glial cell lineages in the rat cerebral cortex. Exp Neurol 1999;156:418–429.
44 Ghaffari M, Whitsett JA, Yan C. Inhibition of hSP-B promoter in respiratory epithelial cells by a dominant negative retinoic acid receptor. Am J Physiol 1999;276:L398–404.
45 Bjorklund S, Almouzni G, Davidson I et al. Global transcription regulators of eukaryotes. Cell 1999;96:759–767.
46 Namihira M, Kohyama J, Semi K et al. Committed neuronal precursors confer astrocytic potential on residual neural precursor cells. Dev Cell 2009;16:245–255.
47 Sanosaka T, Namihira M, Nakashima K. Epigenetic mechanisms in sequential differentiation of neural stem cells. Epigenetics 2009;4:89–92.
48 Gottlicher M, Minucci S, Zhu P et al. Valproic acid defines a novel class of HDAC inhibitors inducing differentiation of transformed cells. EMBO J 2001;20:6969–6978.
49 Faigle R, Liu L, Cundiff P et al. Opposing effects of retinoid signaling on astrogliogenesis in embryonic day 13 and 17 cortical progenitor cells. J Neurochem 2008;106:1681–1698.
50 Donnell AO, Yang SH, Sharrocks AD. MAP kinase-mediated c-fos regulation relies on a histone acetylation relay switch. Mol Cell 2008;29:780–785.
51 Yang L, Lian X, Cowen A et al. Synergy between signal transducer and activator of transcription 3 and retinoic acid receptor-α in regulation of the surfactant protein B gene in the lung. Mol Endocrinol 2004;18:1520–1532.
52 Song MR, Ghosh A. FGF2-induced chromatin remodeling regulates CNTF-mediated gene expression and astrocyte differentiation. Nat Neurosci 2004;7:229–235.

nature neuroscience

Wnt-mediated activation of NeuroD1 and retro-elements during adult neurogenesis

Tomoko Kuwabara[1], Jenny Hsieh[2,9], Alysson Muotri[3,9], Gene Yeo[4], Masaki Warashina[1,8], Dieter Chichung Lie[5], Lynne Moore[6], Kinichi Nakashima[7], Makoto Asashima[1] & Fred H Gage[6]

In adult hippocampus, new neurons are continuously generated from neural stem cells (NSCs), but the molecular mechanisms regulating adult neurogenesis remain elusive. We found that Wnt signaling, together with the removal of Sox2, triggered the expression of NeuroD1 in mice. This transcriptional regulatory mechanism was dependent on a DNA element containing overlapping Sox2 and T-cell factor/lymphoid enhancer factor (TCF/LEF)-binding sites (Sox/LEF) in the promoter. Notably, Sox/LEF sites were also found in long interspersed nuclear element 1 (LINE-1) elements, consistent with their critical roles in the transition of NSCs to proliferating neuronal progenitors. Our results describe a previously unknown Wnt-mediated regulatory mechanism that simultaneously coordinates activation of NeuroD1 and LINE-1, which is important for adult neurogenesis and survival of neuronal progenitors. Moreover, the discovery that LINE-1 retro-elements embedded in the mammalian genome can function as bi-directional promoters suggests that Sox/LEF regulatory sites may represent a general mechanism, at least in part, for relaying environmental signals to other nearby loci to promote adult hippocampal neurogenesis.

In the neurogenic niche of the adult mammalian brain, self-renewing NSCs give rise to committed neuronal progenitors in the subgranular zone (SGZ) of the dentate gyrus[1]. Astrocytes are an essential cell population that defines the SGZ niche and astrocyte-derived factors have instructive effects to promote adult neurogenesis[2,3]. Recently, it has been shown that Wnt3 expression persists in the adult hippocampus and Wnt3 is released by astrocytes to regulate adult neurogenesis *in vitro* and *in vivo*[4]. In the canonical Wnt/β-catenin pathway, the TCF transcription factor transduces Wnt/β-catenin signals to activate downstream target genes[4–9]. However, the target genes of Wnt/β-catenin signaling that are responsible for promoting adult neurogenesis have not been identified. Moreover, the regulatory mechanism underlying Wnt-mediated neuronal differentiation has not yet been elucidated.

NeuroD1 is a proneural basic helix-loop-helix (bHLH) transcription factor that is essential for the development of the CNS, particularly for the generation of granule cells in the hippocampus and cerebellum[10,11]. Environmental signals regulate adult neurogenesis, at least in part, through the activation of NeuroD1 (refs. 12,13). Previously, we found that overexpression of NeuroD is sufficient to promote neuronal differentiation in adult hippocampal neural progenitors[14], whereas deletion of NeuroD results in decreased survival and maturation of newborn neurons[15]. Thus, we hypothesized that astrocyte-derived Wnt signals may directly or indirectly regulate the transcription of NeuroD1 to control the transition of NSCs to committed neuronal progenitors.

The HMG-box transcription factor Sox2 is expressed in embryonic stem cells and most uncommitted cells in the developing CNS[16–18]. Sox2, which can be detected in cells of the mouse blastocyst, maintains precursor cells in a multipotent state[19–21]. During CNS development, Sox2 prevents neurogenesis[22] and forced expression of Sox2 results in the loss of proneural cells[23]. Overexpression of Sox2 in neural progenitor cells derived from embryonic ventricular zone permitted the differentiation of progenitors into astroglia, but it inhibited neurogenesis[24]. Although these analyses indicate that Sox2 is a transcriptional repressor of neuronal target genes during development, the exact nature of Sox2 regulation during adult neurogenesis remains elusive.

Here, we found that the transcriptional activation of NeuroD1 is dependent on canonical Wnt/β-catenin activation and removal of Sox2 repression from the *Neurod1* promoter in a sequence-specific manner. We discovered a previously unknown overlapping DNA-binding site corresponding to Sox2 and TCF/LEF (Sox/LEF) in the *Neurod1* promoter. Using retrovirus gene delivery of Sox2–Cre-GFP (Cre-GFP fusion protein under the control of the *Sox2* promoter, referred to here as $Sox2^{CRE}GFP$) into β-catenin conditional knockout (cKO) mice,

[1]National Institute of Advanced Industrial Science and Technology (AIST), Tsukuba Science City, Japan. [2]Department of Molecular Biology, Cecil H. and Ida Green Center for Reproductive Biology Sciences, University of Texas Southwestern Medical Center, Dallas, Texas, USA. [3]Department Pediatrics/Cellular & Molecular Medicine, School of Medicine, University of California San Diego, University of California San Diego Stem Cell Program, La Jolla, California, USA. [4]Cellular & Molecular Medicine, School of Medicine, University of California San Diego, La Jolla, California, USA. [5]Adult Neurogenesis and Neural Stem Cell Group, Institute of Developmental Genetics, Helmholtz Zentrum München, German Research Center for Environmental Health, Munich-Neuherberg, Germany. [6]Laboratory of Genetics, The Salk Institute, La Jolla, California, USA. [7]Laboratory of Molecular Neuroscience, Graduate School of Biological Sciences, Nara Institute of Science and Technology, Ikoma, Japan. [8]Present address: Cell Biology Research Center, Genome Research Laboratories, Wako Pure Chemical Industries, Ltd., Amagasaki, Hyogo, Japan. [9]These authors contributed equally to this work. Correspondence should be addressed to T.K. (t.warashina@aist.go.jp).

Received 12 March; accepted 22 May; published online 23 August 2009; doi:10.1038/nn.2360

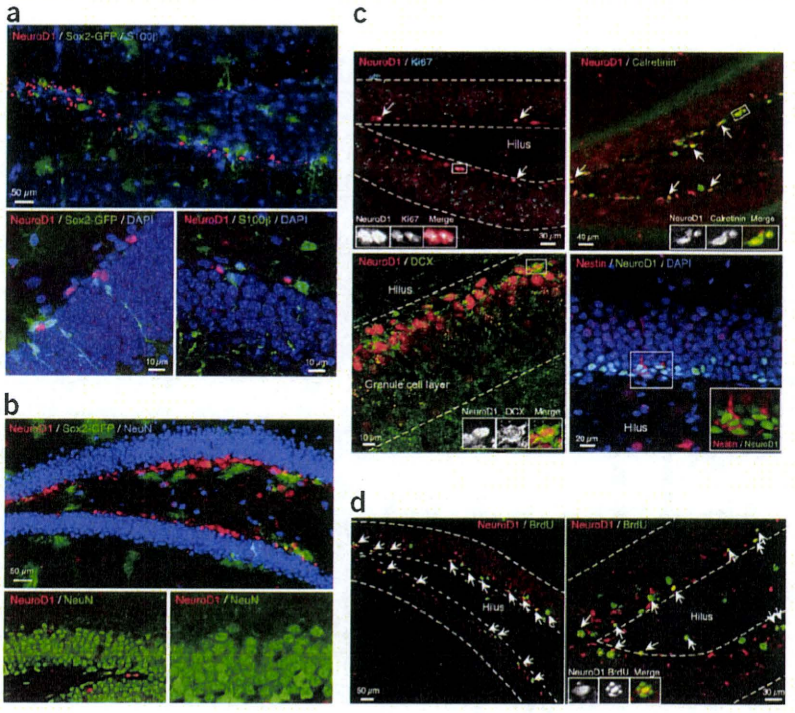

Figure 1 Specific expression of the *Neurod1* gene in early committed neurogenic cells in adult hippocampus. (**a**) Immunohistochemical analysis of neurogenic dentate gyrus area in adult hippocampus of the transgenic mouse that has a *Sox2* promoter–driven EGFP reporter. Top, Sox2 is shown in green, and we stained for NeuroD1 (red) and S100β (blue). Bottom left, a higher-magnification image is shown with DAPI staining (blue) Bottom right, section stained for NeuroD1 (red), S100β (green) and DAPI (blue). (**b**) Distinct population of neuroblast cells expressing the *Neurod1* gene and mature neurons in adult mouse hippocampus. Top, Sox2 is shown in green in adult hippocampus of a *Sox2* promoter–driven EGFP reporter transgenic mouse; we also stained for NeuroD1 (red) and NeuN (blue). Bottom, NeuroD1-positive cells (red) and NeuN-positive cells (green) were exclusive to the inner layer of the dentate gyrus. (**c**) Immunocytochemical analysis of NeuroD1-positive cells in adult rat hippocampus. NeuroD1-positive cells (red) colocalized with Ki67 (cyan). White arrows indicate colocalizing cells; the region in the white square is magnified in a separate window. Bottom left, NeuroD1-positive cells (red) colocalized calretinin (green) and DCX (green). Bottom right, some NeuroD1-positive cells (green) colocalized with nestin (red). White arrows indicate populations of colocalized cells for both markers. (**d**) Proliferative status of NeuroD1-positive cells in adult hippocampus. BrdU (100 mg per kg of body weight) was injected for 1 week into Fisher 344 rats (7–8 weeks old). Cells that were double positive for NeuroD1 (red) and BrdU (green) are indicated by white arrows. The colocalizing cell (NeuroD1 and BrdU positive) in the white square is magnified on the right.

we observed a significant loss ($P < 0.001$; data represent mean ± s.d., $n = 6$ per group) of NeuroD1-positive progenitors as well as a decrease in newborn granule neurons, with no effect on the stem/progenitor cell pool. These findings are extended to the regulation of LINE-1 retrotransposon expression through silencing and activation of Sox2 and Wnt/β-catenin, respectively, which is consistent with LINE-1 being critical during neuronal differentiation[25]. Together, these results suggest that Wnt-mediated activation of NeuroD1 and LINE-1 is coordinately regulated during adult neurogenesis, which may extend to other nearby genomic loci using the bi-directionality of Sox/LEF sites. These findings also suggest that crosstalk between Sox2 and Wnt/β-catenin signaling represents an important mechanism underlying neuronal differentiation.

RESULTS

The expression of Sox2 and NeuroD1 in adult neurogenesis

To characterize the expression of transcription factors in adult dentate gyrus, we performed immunohistochemical analysis in the Sox2–enhanced GFP (EGFP) transgenic mouse[1,26]. NeuroD1-positive cells were clearly detected in the SGZ region of the dentate gyrus and did not colocalize with Sox2-GFP or S100β, a marker of astrocytes (**Fig. 1a**). Moreover, Sox2-positive and NeuroD1-positive cells were mutually exclusive with mature neurons, suggesting that Sox2 and NeuroD1 counteract one another to regulate the early stages of adult neurogenesis (**Fig. 1b**).

To further define the properties of NeuroD1-positive cells, we examined additional markers of stem/progenitor cells and immature granule neurons. NeuroD1-positive cells colocalized with nestin, calretinin and doublecortin (DCX; **Fig. 1c**). Sox2-GFP cells colocalized with the radial glial cell marker nestin, whereas only a few weakly stained GFP-positive cells colocalized with the weaker DCX-positive cells[1]. A majority of the NeuroD1-positive cells colocalized with DCX, whereas only a few cells were nestin positive, suggesting that NeuroD1-positive cells have recently transitioned from Sox2-positive NSCs to neuronal progenitors/immature neurons (**Fig. 1c**). In addition, NeuroD1-positive cells colocalized with Ki67 (**Fig. 1c**), indicating that they are among the proliferating population in adult dentate gyrus. To further examine their proliferative status, we treated Fischer 344 rats with BrdU and found that NeuroD1-positive cells colocalized with BrdU-positive cells in the SGZ (**Fig. 1d**). Taken together, these data indicate that NeuroD1 is transiently expressed in dividing progenitor cells and immature granule neurons in adult dentate gyrus and suggest that the expression of Sox2 and NeuroD1 must be coordinately regulated during adult neurogenesis.

Sox/LEF DNA recognition motif in the *Neurod1* promoter

Next, we surveyed 3 kb of the regulatory region upstream of the *Neurod1* and *Neurod2* promoters and found binding sites for the TCF/LEF and Sox transcription factors (**Fig. 2a**). Notably, some Sox and TCF/LEF sequences were found to overlap with each other, forming a previously unknown binding motif, which we refer to as the Sox/LEF-binding site, that was conserved among humans, rats and mice (**Fig. 2b**).

Using an established adult rat hippocampal NSC line[27], we compared the relative expression levels of *Sox2*, *Neurod1* and other pro-neural genes. Adult NSCs expressed high levels of Sox2 in undifferentiated stages (**Fig. 2c**), but Sox-2 expression was reduced in neurons. In contrast, both NeuroD1 and NeuroD2 were significantly upregulated ($P < 0.001$) in neurons (**Fig. 2c**). Notably, induction levels of NeuroD1 and NeuroD2 were higher than those of Neurog1 and Neurog2, which function as important bHLH proteins during neural development[28–30]. Gene activation by Wnt/β-catenin signaling requires

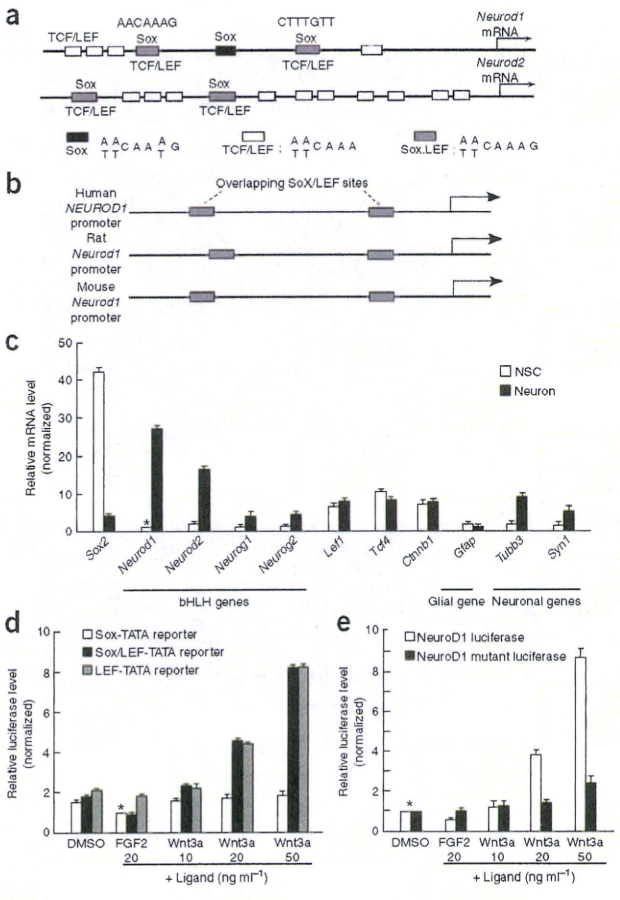

Figure 2 Sox2/LEF DNA regulatory elements on the *Neurod* promoters. (**a**) Schematic representation of the binding sites of TCF/LEF and Sox transcription factors on the 3-kb promoters of the *Neurod1* and *Neurod2* genes. The sequences of the DNA regulatory elements recognized by Sox2 (black box) and TCF/LEF (white box) and the overlapping DNA regulatory consensus sequence (Sox/LEF; gray box) recognized by both Sox2 and TCF/LEF are shown (bottom). (**b**) Schematic representation of the Sox2/LEF-binding sites (gray boxes) in human, rat, and mouse *Neurod1* promoters. (**c**) Comparison of expression levels between NSCs and differentiating neurons by quantitative real-time PCR (qRT-PCR) of genes related to Wnt signaling. The expression level of *Gfap* as a typical glial gene was assessed. Expression levels of β-tubulin III (*Tubb3*) and synapsin I (*Syn1*) were also analyzed as neuronal genes. Each mRNA value was normalized to that of *Gapdh* and then plotted as the fold increase of the sample of *Neurod1* mRNA in NSCs (asterisk). (**d**) Simple reporter assay with the regulatory elements of Sox2, TCF/LEF and Sox/LEF transcription factors. The luciferase value was normalized to a sample with a Sox-TATA reporter construct, with an FGF2 ligand (asterisk). (**e**) Activity of the *Neurod1* promoter. A 1.5-kb *Neurod1* promoter region (including a Sox/LEF site and a TCF/LEF site) was linked to the *luciferase* gene. The reporter construct with mutation at the Sox/LEF site on the *Neurod1* promoter (NeuroD1 mutant luciferase) was also introduced to the adult NSCs. Luciferase value was normalized to sample with DMSO as a control ligand (asterisk).

stabilization of the β-catenin protein and nuclear association with TCF/LEF[9]. We found that the mRNA levels of β-catenin, TCF and LEF1 remained unchanged during neuronal differentiation, suggesting that Wnt and β-catenin are regulated at the post-transcriptional level (**Fig. 2c**).

To investigate the requirement of the Sox/LEF sequence, we prepared a set of reporter constructs (Sox-, Sox/LEF- and LEF-TATA; Online Methods). Incubation with fibroblast growth factor 2 (FGF2), which maintains cells in an undifferentiated state, reduced luciferase activity resulting from the Sox-TATA and Sox/LEF-TATA constructs, but not from the LEF-TATA construct, compared with the luciferase activity in cells treated with DMSO. This finding suggests that the Sox regulatory element has a negative role on transcription in the presence of FGF2, whereas the LEF regulatory element itself has no effect. When the Wnt3a ligand was introduced to cells, we observed a clear dose-dependent upregulation of luciferase in cells expressing the Sox/LEF-TATA and LEF-TATA constructs (**Fig. 2d**). The Sox regulatory element itself had almost no effect in the presence of Wnt3a, indicating that there is an apparent functional difference in the Sox and LEF regulatory elements with regard to ligand response.

Next, we introduced the Wnt3a ligand into NSCs and observed a dose-dependent upregulation of *Neurod1* promoter activity (**Fig. 2e**). In contrast, when the mutant reporter construct (NeuroD1 mutant luciferase (**Fig. 2e**) contains a mutation in the Sox/LEF site to abolish Sox2 and TCF/LEF binding) was introduced into NSCs, we failed to observe either a reduction in luciferase activity in the undifferentiated state (FGF2 ligand) or an increase in luciferase activity by the addition of Wnt3a ligand (**Fig. 2e**). These data suggest that the Sox/LEF binding sequence in the *Neurod1* promoter is important for discriminating between both TCF/LEF- and Sox2-mediated transcriptional regulation during adult neurogenesis.

Upregulation of NeuroD1 is dependent on the Sox/LEF site

To investigate the regulatory mechanism underlying *Neurod1* gene transcription, we compared the expression of NeuroD1 with that of proteins in the Wnt signaling pathway. S100β-positive and glial fibrillary acidic protein (GFAP)-positive astrocytes were also positive for both Wnt3 and Wnt3a, consistent with published results[4] (**Supplementary Fig. 1**). Following neuronal differentiation *in vitro*, NeuroD1 expression peaked at 1 d after neuronal induction and diminished by 4 d. In protein blotting experiments, we found that Sox2 was expressed in undifferentiated NSCs and downregulated on neuronal differentiation (**Fig. 3a**). In contrast, β-catenin was clearly stabilized and accumulated when NeuroD1 was highly expressed, although the level of β-catenin mRNA was unchanged (**Fig. 2c**). These results suggest that NeuroD1 expression is temporally regulated, consistent with NeuroD1 expression *in vivo*, and Wnt/β-catenin activation and de-silencing of Sox2 may be involved in promoting neuronal differentiation.

For Wnt-mediated transcriptional activation of target genes, the phosphorylated, inactive form of GSK3β is the canonical enhancer for the stabilization of β-catenin protein[9]. Thus, we assessed whether neuronal differentiation in adult NSCs influenced the phosphorylation of GSK3β. As hypothesized, GSK3β phosphorylation was triggered on neuronal differentiation, whereas total GSK3β levels remained unchanged (**Fig. 3b**).

To evaluate the effects of Wnt signaling on *Neurod1* gene activity, we carried out gain-of-function studies using Wnt3a-expressing lentivirus[4] and a pharmacological inhibitor of GSK3β (TDZD8). For loss-of-function studies, we used a full-length cDNA *Sox2* construct, a secreted mutant Wnt (dominant-negative Wnt, DnWnt) construct[4], a small hairpin RNA (shRNA) that was specific to β-catenin mRNA (**Supplementary Fig. 2**) and the Wnt antagonist Dickkopf1 (Dkk1). *Neurod1* mRNA levels were strongly increased by both Wnt3a expression and the GSK3β inhibitor (**Fig. 3c**). In contrast, Dkk1, DnWnt and an shRNA to β-catenin reduced NeuroD1 expression. To further examine the effect of Wnt3a expression on NeuroD1 transcriptional activation, we introduced a NeuroD1 luciferase construct into adult

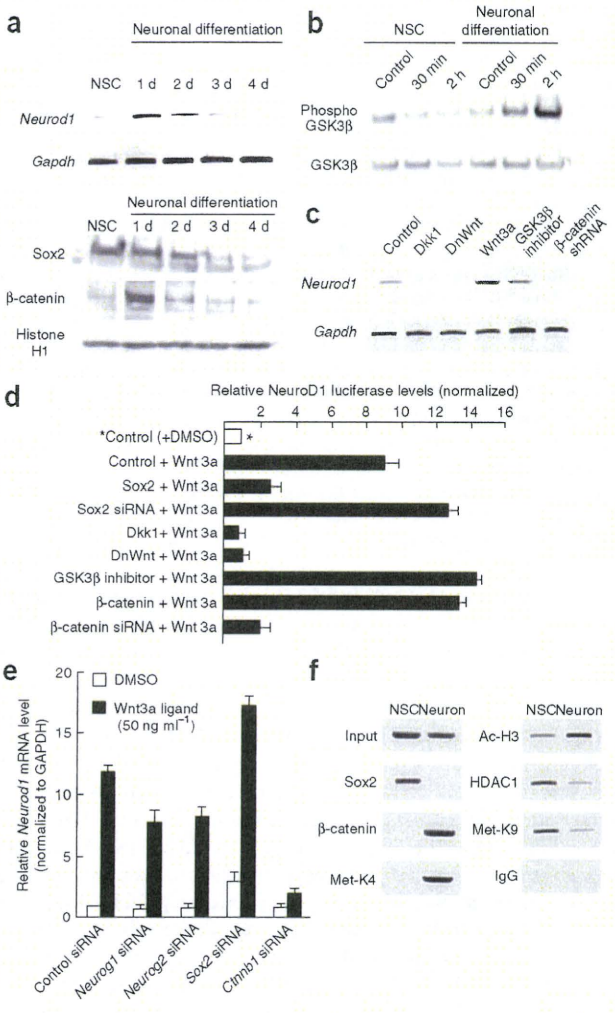

Figure 3 Wnt signaling increases *Neurod1* promoter activity during early neurogenesis. (**a**) Time course of *Neurod1* mRNA expression during the early stages of neurogenesis in cultured adult NSCs. RT-PCR detection of *Neurod1* and *Gapdh* is shown. Western blots of Sox2 and β-catenin during neurogenesis in cultured adult NSCs are shown in the lower panels. (**b**) Induction of a phosphorylated inactive form of GSK3β to stabilize β-catenin during Wnt signaling in early committed neurogenic cells. Western blots of both GSK3β and phosphorylated GSK3β were conducted using the same neuronal induction treatment. (**c**) The effect of Wnt signaling on the expression of *Neurod1* mRNA. RT-PCR analysis using total RNA extracted from adult NSCs treated with Dkk1, DnWnt, Wnt3, TDZD8 or β-catenin shRNA. (**d**) The effect of Wnt signaling on the promoter activity of the *Neurod1* gene. The luciferase value was normalized to that of cultured NSC sample with control vector and control ligand (DMSO, asterisk, white bar). (**e**) The effect of siRNAs targeting Neurog1, Neurog2, Sox2 and β-catenin on Wnt3a ligand–mediated induction on *Neurod1* mRNA. qRT-PCR analysis for *Neurod1* mRNA was plotted. The amount of mRNA present for each sample was normalized to that of *Gapdh* and then plotted as the fold increase over the control (control siRNA with DMSO). (**f**) ChIP analysis at the *Neurod1* promoter in adult neurogenesis. PCR primers were designed to surround the Sox/LEF sequence on the rat *Neurod1* promoter.

NSCs. Sox2, Dkk1 and DnWnt expression all had negative effects on Wnt3a-mediated NeuroD1 transcriptional activation. In contrast, *Neurod1* promoter activity was further enhanced by the constitutively active form of β-catenin and by TDZD8 (**Fig. 3d**).

To confirm that the transcriptional activation of NeuroD1 is dependent on the Wnt3a ligand, we introduced several sets of synthesized small interfering RNAs (siRNAs) into adult NSCs. Wnt3a ligand increased *Neurod1* mRNA expression (~12-fold increase) in control siRNA-transfected cells (**Fig. 3e**). In contrast, β-catenin siRNA substantially reduced NeuroD1 activation on Wnt3a ligand treatment (~sixfold decrease). Notably, we did not observe substantial reduction of Wnt3a-mediated NeuroD1 activation by Neurog1 and Neurog2 siRNAs, indicating that Wnt3a effects on NeuroD1 may be direct. The amount of NeuroD1 mRNA increased in cells treated with Sox2 siRNA more than in cells treated with control siRNA, possibly as a result of residual endogenous Sox2 protein at the onset of neuronal induction (**Fig. 3a**), which may have a negative influence on NeuroD1 expression.

Finally, we performed chromatin immunoprecipitation (ChIP) analysis to assess protein association. We found that Sox2 and the histone deacetylase HDAC1 repressor protein were associated on the endogenous *Neurod1* promoter, specifically at the Sox/LEF site, in undifferentiated NSCs, and that this association diminished when the neurons differentiated (**Fig. 3f**). Consistently, di-methylated histone H3 at Lys9 (K9), commonly associated with transcriptional repression[31], was also present in NSCs. Moreover, β-catenin, acetylated histone H3 and methylated histone H3 at Lys4 (K4), all of which are associated with transcriptional activation, were observed on the *Neurod1* promoter locus in neuronal cells, suggesting that *Neurod1* gene transcription is mediated by an active process. These results suggest that the conversion of a Sox2 repressor complex to a β-catenin activator complex is associated with chromatin remodeling on neuronal induction.

Wnt3a-dependent activation of LINE-1 retrotransposon

Sox2 can suppress LINE-1 expression in adult NSCs[25]. The observation that Sox2 is downregulated at nearly the same time that β-catenin is upregulated raises the possibility that they may target the same Sox/LEF regulatory sequences in neuronal genes. Indeed, many Sox/LEF-binding sites were present throughout the entire LINE-1 sequence, including several sites in open reading frame 2 (ORF2; **Fig. 4a**). We next determined whether these sequences were functional using reporter assays in adult NSCs.

We previously reported that promoter activity in the human LINE-1 5′ untranslated region (UTR) is increased during neuronal differentiation compared with undifferentiated cells[25]. We confirmed this observation using a reporter construct containing the LINE-1 5′ UTR in both forward and reverse orientation upstream of the *luciferase* gene (**Fig. 4b**). Because ORF2 of LINE-1 contains several Sox/LEF-binding sites, we cloned the LINE-1 ORF2 portion and linked it to the *luciferase* gene to assess putative promoter activity. The ORF2 sequence demonstrated promoter activity in both forward and reverse orientation during neuronal differentiation. The activity was highest 1 d after neuronal induction and it gradually declined during neuronal differentiation. This transient upregulation immediately after neuronal induction was common to both LINE-1 5′ UTR– and ORF2-based reporter constructs (**Fig. 4b**), a finding that is also consistent with the expression dynamics of NeuroD1 (**Fig. 3a**).

LINE-1 sequences comprise a substantial part of the genome, and because the Sox/LEF sites are clustered in LINE-1 sequences, they are also prevalent in the genome. Using ChIP, we found that Sox2 and HDAC were associated in undifferentiated NSCs in which LINE-1 was silenced (**Fig. 4c**), similar to their association on the *Neurod1* promoter (**Fig. 3f**). On the other hand, we observed that β-catenin and acetylated histone H3 associated with each other in neurons. To investigate Wnt3a

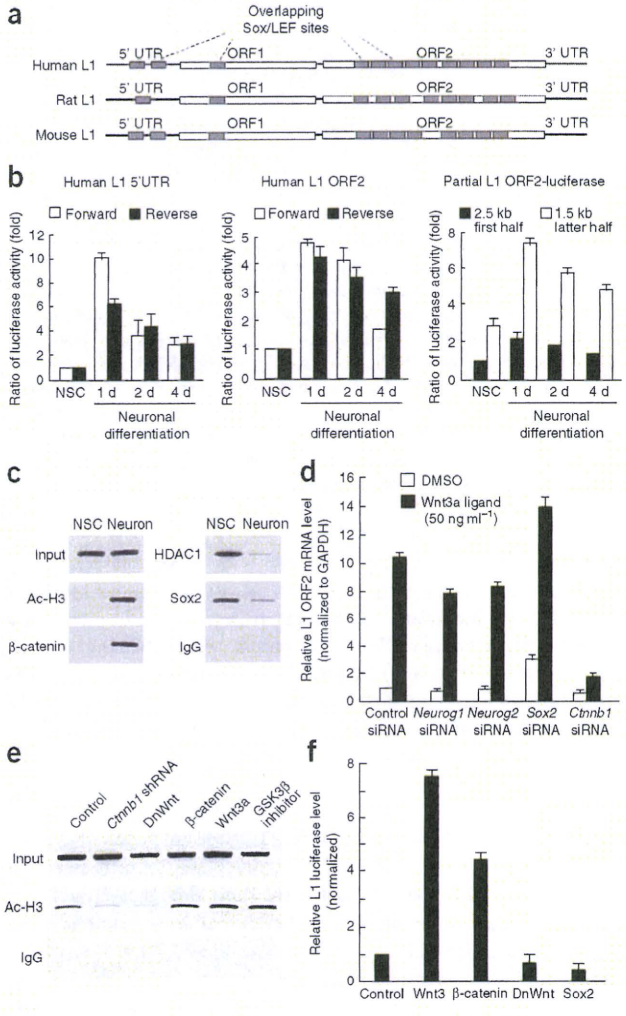

Figure 4 Effect of Wnt signaling on the expression of NeuroD1 and LINE-1 during adult neurogenesis. (**a**) DNA regulatory elements recognized by Sox2 and TCF/LEF transcription in LINE-1. A schematic representation of the Sox/LEF DNA regulatory elements (gray boxes) in the human, rat, and mouse retrotransposon LINE-1 is shown. (**b**) Promoter activity of the 5′ UTR and ORF fragment of LINE-1 during adult neurogenesis. Luciferase constructs with 5′ UTR and LINE-1 ORF2 sequences linked to the *luciferase* gene, in both forward (white) and reverse (black) orientations, were introduced into adult NSCs by lentivirus infection (left and middle panels). Partial fragments of the LINE-1 ORF2, the first 2.5 kb (black columns) and the last 1.5 kb (white columns), were also linked to the *luciferase* gene in the reporter assay (right). (**c**) ChIP analysis of rat LINE-1. PCR primers were designed to surround the Sox/LEF DNA regulatory elements. (**d**) Wnt3a-mediated induced production of LINE-1 ORF2 mRNA. The induction level was measured by qRT-PCR with several synthesized siRNAs. The mRNA level was normalized to that of *Gapdh* and then plotted as the fold increase over the control (control siRNA with DMSO). (**e**) The effect of Wnt signaling on the chromatin remodeling of LINE-1. Activation of the chromatin state (acetylation of histone H3) in the LINE-1 sequences was assessed using several Wnt-related constructs. (**f**) The activation and repression of the LINE-1 promoter. The effect of Wnt on the activity of LINE-1–based promoters was examined using the LINE-1 luciferase construct. After 1 d in the culture, luciferase assays were performed on adult NSCs treated with each construct.

ligand–mediated transcriptional activation of LINE-1 mRNAs, we compared the induction levels of LINE-1 in cells given control siRNA with the cells treated with several gene-specific siRNAs. Wnt3a ligand caused a tenfold increase in the amount of LINE-1 ORF2 mRNA in cells treated with control siRNA (**Fig. 4d**). When cells were treated with β-catenin siRNA, Wnt3a ligand–induced activation was almost abolished, whereas treatment with Neurog1 and Neurog2 siRNAs had almost no effect on Wnt3a-mediated stimulation. On introduction of Sox2 siRNA, endogenous LINE-1 was upregulated and Wnt3a-mediated stimulation of LINE-1 was increased (**Fig. 4d**).

Next, we examined the chromatin status (acetylated histone H3) in the LINE-1 element. β-catenin shRNA and DnWnt stopped the chromatin from switching from the silenced state to the activated state (**Fig. 4e**). The expression of endogenous LINE-1 mRNA was also downregulated by β-catenin shRNA (**Supplementary Fig. 2**), consistent with our ChIP data. The addition of Wnt3, β-catenin or TDZD8 increased acetylated histone H3 levels in the LINE-1 genomic region, indicating that Wnt signaling itself could induce the active chromatin state, directly or indirectly, in the LINE-1 locus (**Fig. 4e**).

We also examined the effect of Wnt3a on the activity of LINE-1–based promoters using the LINE-1 luciferase construct. β-catenin and Wnt3a enhanced LINE-1 luciferase activity significantly ($P < 0.001$) (**Fig. 4f**). In contrast, Sox2 and DnWnt did not promote LINE-1–promoter activity. These results suggest that Wnt signaling actively mediates the expression of LINE-1 in neurons and that the process is not merely a result of de-repression of LINE-1 transcription.

Because LINE-1 sequences are spread throughout the genome, we decided to investigate which genes might be under the influence of this molecular mechanism. Using computational analysis, we scanned downstream regions of human genes that were likely to influence transcription, looking for LINE-1 sequences that contained Sox2, LEF or Sox/LEF-binding sites. We identified 79, 84 and 25 LINE-1 elements within −6,000 and +1,000 base pairs of the start sites of the human, mouse and rat genes, respectively (**Supplementary Tables 1–3**). The LINE-1 elements from different species were not consistently near the same genes. Notably, we found genes encoding olfactory receptors in mouse containing Sox/LEF-binding sites upstream of LINE-1 elements. Furthermore, and of particular interest to us, we found several neuronally relevant genes that may be susceptible to the repressor/activator mechanism described above, including, for example, DCX and Neuregulin 4, or related to cell cycle (SCAPER (zinc finger protein 291) and mitogen-activated protein kinase 10; **Supplementary Tables 1–3**).

Role of β-catenin in neuronal differentiation of adult NSCs

We further investigated the effect of Wnt/β-catenin signaling on cell fate choice *in vivo*. A retrovirus encoding *Sox2* promoter–driven *cre-gfp* ($Sox2^{CRE}GFP$)[1] was injected into the dentate gyrus of $Ctnnb1^{loxP/loxP}$ mice (β-catenin cKO; **Supplementary Fig. 3**)[32]. Because a retrovirus only transduces one of the two daughter cells of dividing cells, single-cell clones are generated by the conversion of Sox2-positive cells to differentiated lineages in β-catenin cKO mice.

To identify the composition of cell types in the Sox2 lineage, we carried out an immunohistochemical analysis (**Figs. 5** and **6**). The number of total GFP-positive cells in β-catenin cKO mice was decreased by about 50% compared with control mice (**Fig. 5b**). In control mice, many $Sox2^{CRE}$GFP-positive cells colocalized with NeuroD1-positive cells (**Fig. 5a**). In contrast, the proportion of ND1 and GFP double-positive cells in β-catenin cKO mice was decreased by 92% relative to that of control mice (**Fig. 5c,d**). In addition to NeuroD1, $Sox2^{CRE}$GFP-positive cells that colocalized with markers for newborn neurons, such as DCX (**Supplementary Fig. 4**) and TUJ1 (**Supplementary Fig. 5**), were

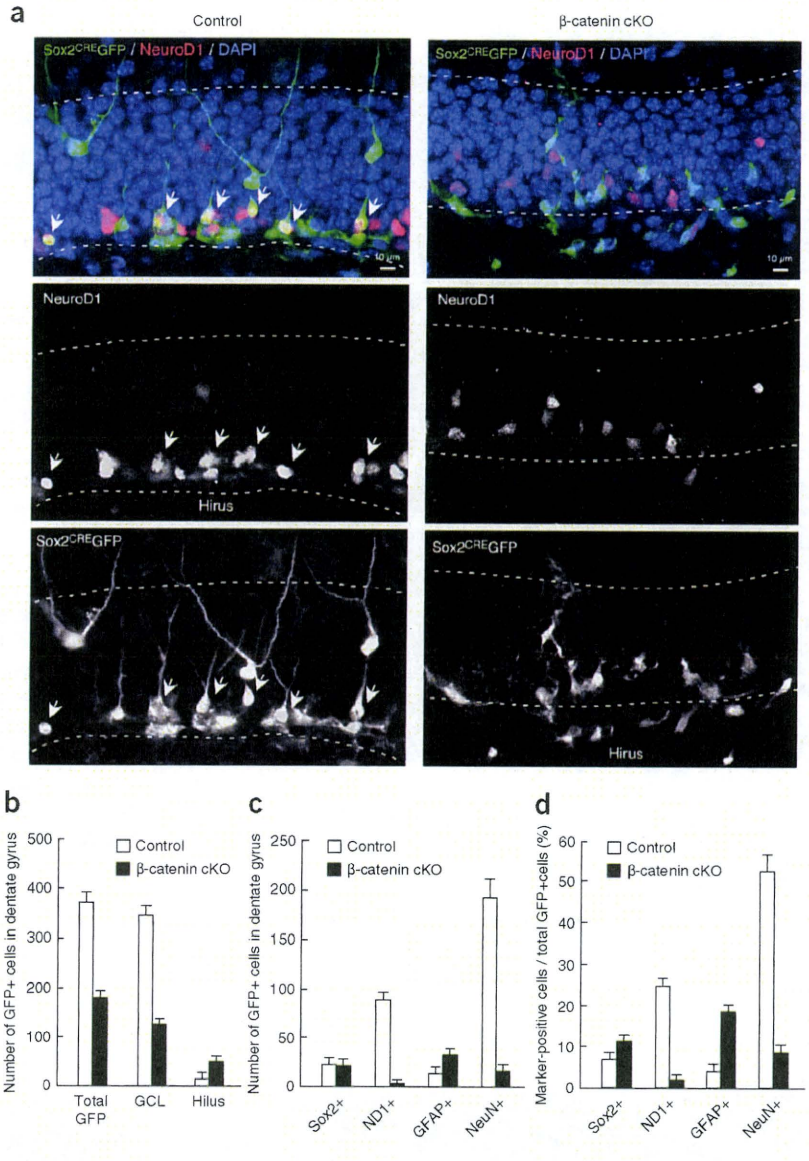

Figure 5 Adult NSC cannot transition to immature and mature granule neurons in β-catenin cKO mice. Immunohistochemical analysis of the Sox2^{CRE}GFP cells. (**a**) Sox2^{CRE}GFP retrovirus was injected into the dentate gyrus of control mice (left) or β-catenin cKO mice (right). Immunohistochemical analysis of NeuroD1 (red), GFP (green) and DAPI (blue) in both groups is shown and GFP-positive cells colocalized with NeuroD1-positive cells in control mice (indicated by white arrows, left panels). In control mice, GFP-positive cells were present among the more differentiated neurons deeper in the granule cell layer (left). In β-catenin cKO mice, GFP-positive cells were observed more often near or in the hilus region, rather than among the more differentiated neurons deeper in the granule cell layer. (**b**) Numbers of GFP-positive cells in the dentate gyrus of control mice (white bars) and β-catenin cKO mice (black bars). (**c**) Numbers of marker and GFP double-positive cells in the dentage gyrus of control mice (white bars) and β-catenin cKO mice (black bars). (**d**) Percentages of marker-positive cells in the dentage gyrus of control mice (white bars) and β-catenin cKO mice (black bars).

significantly reduced ($P < 0.001$) in the β-catenin cKO mice (**Supplementary Fig. 6**). In control mice, we readily observed Sox2^{CRE}GFP-positive cells that gave rise to mature neurons with extensive neurites (**Fig. 5a**). Quantification of Sox2^{CRE}GFP-positive cells in control mice revealed that ~50% of them became NeuN-positive mature granule neurons (**Fig. 5d**).

In contrast, there was a substantial decrease in Sox2^{CRE}GFP-positive cells that became mature neurons in β-catenin cKO mice (**Fig. 5a**). The percentage of NeuN and GFP double-positive cells was reduced by 85% relative to that of control mice (**Fig. 5d**). The number of Sox2^{CRE}GFP-positive cells that were also labeled by Prox-1, which labels both immature and mature neurons, was also reduced by 90% in β-catenin cKO mice compared with control mice (**Supplementary Fig. 6**).

To examine Sox2^{CRE}GFP-positive cells in the stem cell compartment, we stained the cells with GFAP, a marker of radial stem-like cells and astrocytes, and BrdU (**Fig. 6a**). The proportion of GFAP and GFP double-positive cells in β-catenin cKO mice was 4.4-fold higher than that in control mice (**Fig. 5d**). The Sox2-^{CRE}GFP-positive cells in β-catenin cKO mice were also positive for Sox2 and labeled with BrdU (**Fig. 6b**). There was no substantial change in the number of GFP and Sox2 double-positive cells (**Fig. 5c**). The proportion of GFP and Sox2 double-positive cells was 1.5-fold higher than that in control mice (**Fig. 5d**).

We observed similar results with a lentivirus approach *in vivo*. Cells that were positive for the lentivirus encoding β-catenin shRNA and GFP cells did not significantly colocalize with NeuroD1-positive cells ($P < 0.001$), whereas control lentivirus-GFP–positive cells colocalized with many NeuroD1-positive cells (**Fig. 7** and **Supplementary Fig. 7**). Cells infected with a lentivirus expressing shRNA specific to β-catenin were positive for Sox2 and BrdU, similar to cells infected with a control lentivirus expressing GFP (**Supplementary Fig. 8**). The shRNA-GFP–positive cells colocalized with GFAP-positive cells and Nestin-positive cells (Nestin is a radial glial cell marker) (**Supplementary Fig. 9**). These data suggest that the maintenance of the undifferentiated stem cell compartment and, to a large extent, astrocytic lineage cells and/or GFAP-positive radial stem-like cells remained intact with knockdown of β-catenin. Together, these data indicate that Sox2-positive cells cannot transition to immature and mature granule neurons when Wnt/β-catenin signaling is blocked, whereas the stem/progenitor cell compartment remains intact.

Wnt is important for survival of neuronal progenitor cells

The decrease of Sox2^{CRE}GFP-positive cells in β-catenin cKO mice could also be explained by a defect in the survival of neuronal progenitors. Thus, we examined the presence of dead and/or dying cells by activated caspase 3 (AC3) staining. We found more AC3-positive cells in dentate gyrus of β-catenin cKO mice than in control mice (**Fig. 6c,d**). Although we observed AC3-positive cells that colabeled

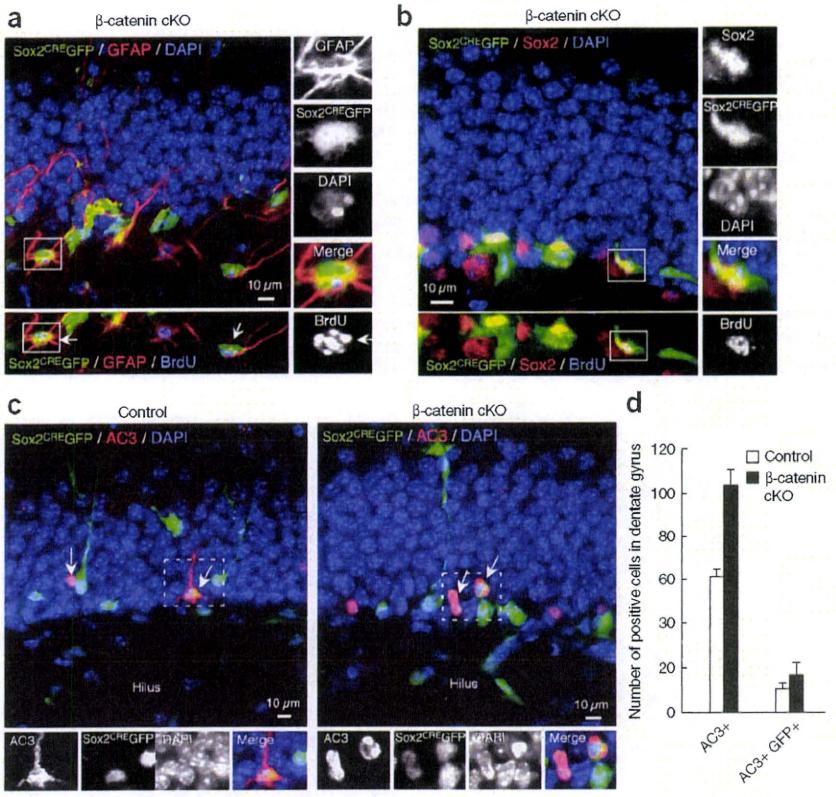

Figure 6 Lineage tracing Sox2-positive NSCs in β-catenin cKO mice. Immunohistochemical analysis of the Sox2^{CRE}GFP cells. (**a**,**b**) Sox2-positive cells were able to give rise to GFAP-positive (red, **a**) and to Sox2-positive NSCs (red, **b**). Magnified images show triple immunohistochemistry of GFAP (**a**) or Sox2 (**b**), GFP (green) and BrdU (blue, lower panels). (**c**) Immunohistochemical analysis of apoptotic cells labeled by AC3 in β-catenin cKO mice. Representative image of AC3 (red), GFP (green) and DAPI (blue) in control mice (left) and β-catenin cKO mice (right). The GFP-positive cells colocalizing with the AC3-positive cells are indicated by white arrows. The GFP and AC3 double-positive cells in the white dotted square are magnified in the bottom panels. (**d**) Quantification of GFP-positive and AC3-positive cells in dentate gyrus of control and β-catenin cKO mice. The numbers of the AC3-positive and AC3 and GFP double-positive cells in the dentate gyrus of control mice (white bars) and β-catenin cKO mice (black bars) are plotted.

with Sox2 (**Supplementary Fig. 10**), the total number of Sox2-positive cells remained unchanged in β-catenin cKO mice (**Fig. 5c**), suggesting that inhibition of Wnt/β-catenin signaling in Sox2-positive NSCs is important for the generation NeuroD1-positive cells from Sox2-positive NSCs, as well as for the survival of neuronal progenitors.

Finally, to examine whether Wnt/β-catenin–mediated neuronal differentiation is dependent on NeuroD1, we performed loss-of-function experiments in adult NSCs expressing siRNA specific to NeuroD1, as well as in subventricular zone and dentate gyrus neurospheres from 4-week-old *Neurod1*$^{loxP/loxP}$ mice (NeuroD1 cKO) mice[15]. The addition of Wnt3a ligand induced microtubule associated protein 2AB (Map2AB) expression in neurons in NSCs that were treated with of control random siRNA; Map2AB expression was completely suppressed with the introduction of NeuroD1 siRNA (**Supplementary Fig. 11**). Moreover, Wnt3a ligand treatment in NeuroD1 cKO neurospheres[15] with control GFP lentivirus resulted in TUJ1-positive neurons after 2 d (**Supplementary Fig. 12**). However, in the presence of lentivirus expressing Cre, which caused the deletion of NeuroD1, Wnt3a stimulation failed to induce substantial numbers of TUJ1-positive neurons, which is consistent with the idea that NeuroD1 is essential for Wnt3a-mediated neuronal differentiation.

LINE-1 promoter activity in newborn and mature neurons

On the basis of our results, we hypothesized that LINE-1 sequences are active during adult neurogenesis. To evaluate LINE-1–based promoter activity *in vivo*, we prepared a lentiviral vector that encodes the LINE-1

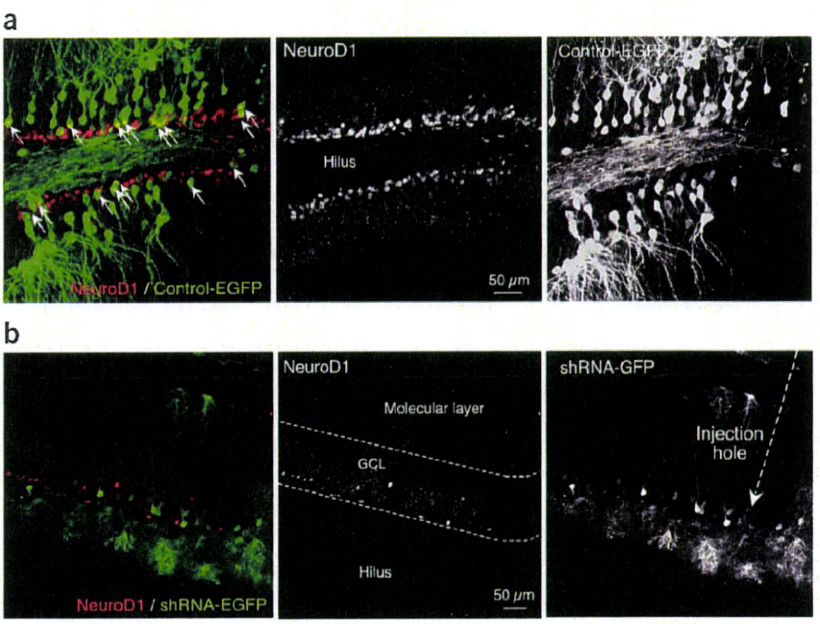

Figure 7 Infection of lentivirus expressing β-catenin shRNA *in vivo*. To evaluate the effect of Wnt signaling *in vivo*, lentivirus expressing β-catenin shRNA or control lentivirus expressing only EGFP (lentivirus-GFP) was stereotactically injected into adult rat hippocampus. (**a**) Lentivirus-GFP in dentate gyrus. White arrows indicate the population of cells that were double positive for NeuroD1 (red) and EGFP (green). (**b**) Immunohistochemical analysis of the cells infected by the lentivirus encoding β-catenin shRNA and GFP. Cells expressing β-catenin shRNA and GFP (green) and NeuroD1-positive cells (red) are shown.

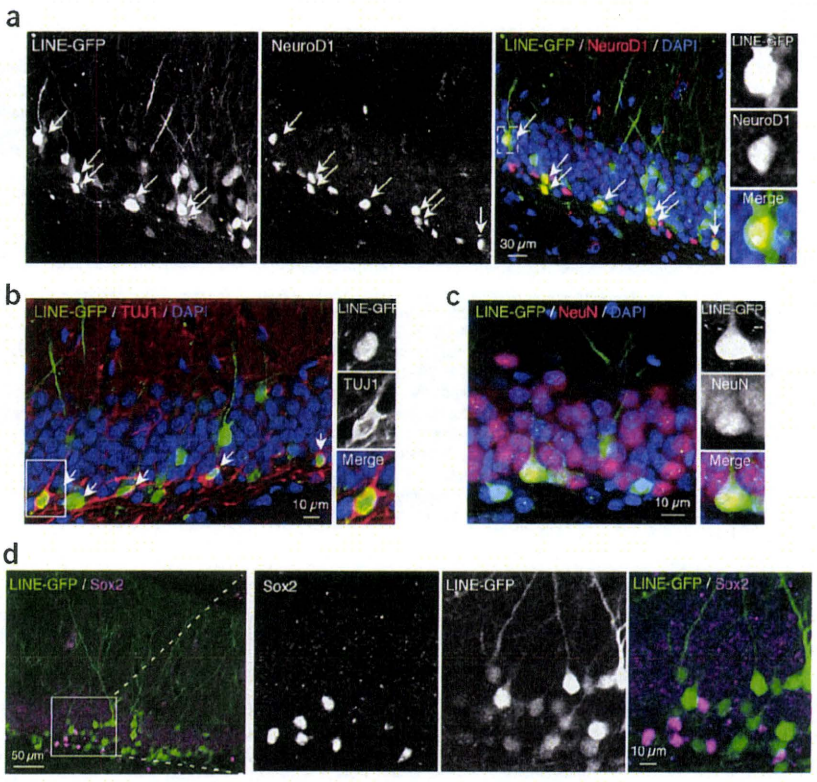

Figure 8 Activity of LINE-1 as a promoter in adult rat hippocampus. (**a**–**d**) We examined the activity and specificity of the LINE-1–based promoter in adult rat hippocampus. EGFP-expressing lentivirus, under the control of the LINE-1–based promoter, was stereotactically microinjected into the dentate gyrus of adult rats and the population of GFP-positive cells (green) was analyzed by immunohistochemistry using an antibody to NeuroD1 (red, **a**). Comparisons of the LINE-GFP population (green) to TUJ1 staining (red, **b**), NeuN staining (red, **c**) and Sox2 staining (magenta, **d**) are also shown.

ORF2 fragment fused to the *egfp* gene (LINE-GFP). LINE-GFP lentivirus was stereotactically injected into dentate gyrus of young adult rats. Notably, we observed LINE-GFP expression restricted to neurogenic areas, and GFP-positive cells colocalized with NeuroD1-positive neuronal progenitors and TUJ1-positive newborn granule neurons (**Fig. 8a,b**). Moreover, we observed a similar expression pattern of the 5′ UTR of LINE-GFP in TUJ1-positive newborn neurons in dentate gyrus (**Supplementary Fig. 13**). We also detected LINE-GFP–positive cells that migrated further into the granule cell layer, where mature neurons reside that were NeuN positive[33] (**Fig. 8c** and **Supplementary Fig. 14**). LINE-GFP–positive cells were negative for Sox2 (**Fig. 8d**). These *in vivo* data are consistent with our *in vitro* results, which indicate that NeuroD1 and LINE-1 expression are specifically induced only when Sox2-positive NSCs transition to newborn neurons on Wnt/β-catenin activation.

DISCUSSION

We found an important function for canonical Wnt/β-catenin signaling in balancing self-renewal of NSCs and neuronal differentiation in adult dentate gyrus. Our results (as summarized in **Supplementary Fig. 15**) indicate that the Sox2 and TCF/LEF regulatory element in the *Neurod1* promoter is critical for the transition from Sox2-mediated repression to Wnt/β-catenin-mediated activation, that the clear, dose-dependent activation of the *Neurod1* promoter by the Wnt3a ligand is dependent on the Sox/LEF-binding site, that deletion of β-catenin leads to substantial loss of NeuroD1-positive cells, whereas the stem cell compartment remains intact *in vivo*, and that Wnt/β-catenin–mediated neuronal differentiation is dependent on NeuroD1, at least *in vitro*. Taken together, these findings indicate that the decreased adult neurogenesis observed in the *Sox2–cre-gfp; Ctnnb1*$^{loxP/loxP}$ mice is probably a result of a failure of neuronal lineage commitment from Sox2-positive NSCs and of survival of Sox2- and NeuroD1-positive progenitor cells/neuroblasts.

During embryonic development, neurogenins function as pro-neural proteins that activate transcription of *Neurod1* through E-protein binding sites in its promoter[28–30]. However, the transcriptional/epigenetic mechanism that regulates NeuroD1 expression in the adult neurogenic niche is not clear. In the SGZ, hippocampal astrocyte–derived factors, such as Wnt proteins, signal to NSCs to promote adult neurogenesis. Among several Wnt proteins (Wnt3a, Wnt2a, Wnt5a, Wnt7a and Wnt8b)[34–36], Wnt3a has a dominant role in CNS development, as the deletion of Wnt3a (*Wnt3a*$^{-/-}$ mice) results in the absence of dentate gyrus formation[35]. Furthermore, it has been reported that β-catenin is involved in the dendritic development of newborn neurons[37]. Both canonical[4–8] and noncanonical[37] Wnt/β-catenin signaling may contribute to the step-wise progression of adult hippocampal neurogenesis by removing Sox2 repression and turning on NeuroD1. Similar to a loss of Wnt/β-catenin signaling, NeuroD1 deficiency during hippocampal development leads to a complete loss of dentate gyrus formation in mice[10,11]. In adult stages, when the hippocampal formation is fully developed, conditional deletion of β-catenin and NeuroD1 (ref. 15) lead to a similar phenotype in dentate gyrus, that is, a decreased number of neuronal progenitors/newborn neurons, suggesting that the regulation of canonical Wnt/β-catenin signaling and *Neurod1* gene expression are tightly linked and the functions of both β-catenin and NeuroD1 are indispensable for adult neurogenesis and for the survival of neuronal progenitors. Recently, it was shown that Wnt-mediated adult hippocampal neurogenesis contributed to learning and memory in rats[38]. Our data suggest that Wnt signaling activation might be a major environmental factor that is relayed to the NSC genome for neuronal lineage commitment to modulate behavior.

Our finding that the Wnt-mediated regulatory mechanism is required for the activation of NeuroD1 can be broadly extended to the regulation of LINE-1. Because retro-element sequences are scattered throughout the genome and contain Sox/LEF DNA regulatory elements, one possibility is that Sox/LEF-binding sites act as bi-directional promoters and cause nearby neuronal gene loci to become de-silenced and activated during adult neurogenesis. Thus, to explore the possibility that LINE-1 sequences containing Sox2 and TCF/LEF sites might confer cell type–specific regulation as described for NeuroD1, we searched for LINE-1 sequences proximal to the transcriptional start sites of known protein-coding genes in human, mouse and

rat genomes. We were able to identify 79, 84 and 25 such LINE-1 elements within −6,000 and +1,000 base pairs of the target human, mouse and rat genes, respectively (**Supplementary Tables 1–3**). These bioinformatics analyses suggest that there is a global regulatory mechanism for controlling the activation/repression of neuronal gene expression that uses embedded retrotransposition sequences in the genome as a putative master regulatory pathway during adult neurogenesis. However, the causal relationship between LINE-1 sequences and transcriptional activation of nearby Sox/LEF-driven neuronal genes awaits future validation. Recently, it has been shown that environment is a robust stimulator of adult neurogenesis[39], possibly through the activation of the Sox/LEF regulatory elements described here. Consistent with these data, we recently observed that voluntary exercise increased LINE-1 retrotransposition in dentate gyrus[40]. Our data provides a window into the molecular mechanism behind experience-dependent LINE-1 retrotransposition that may affect neuronal plasticity.

METHODS

Methods and any associated references are available in the online version of the paper at http://www.nature.com/natureneuroscience/.

Note: Supplementary information is available on the Nature Neuroscience website.

ACKNOWLEDGMENTS

We thank T. Ohtake for assistance with animal care and supporting our *in vivo* experiments. We thank M. Namihira and J. Kohyama for assistance in obtaining immunostaining data, E. Mosser for the constitutively active β-catenin construct, and G. Canettieri and M. Montminy for HDAC1. We thank A. Huynh for help with immunohistochemical analysis. We are grateful for the technical assistance of B. Miller and to M.L. Gage for editorial comments. T.K., M.W. and M.A. were supported by various grants from National Institute of Advanced Industrial Science and Technology. T.K. was partly supported by the Grant-in-Aid for Exploratory Research. F.H.G. was supported by grants from the US National Institutes of Health (MH082070) and the G. Harold and Leila Y. Mathers Charitable Foundation.

AUTHOR CONTRIBUTIONS

T.K., J.H., A.M., K.N. and F.H.G. conceptualized and designed the study. T.K., J.H., A.M. and F.H.G. analyzed the data. T.K. conducted the experiments with assistance from M.W., J.H. and L.M. G.Y. and A.M. conducted the bioinformatics analysis. A.M. helped design the LINE-1 plasmid constructs, D.C.L. helped with the Wnt plasmid design and constructs, and M.W. designed the shRNA construct. M.A. contributed reagents and analytical tools. T.K. wrote the paper with comments from all of the authors.

Published online at http://www.nature.com/natureneuroscience/.
Reprints and permissions information is available online at http://www.nature.com/reprintsandpermissions/.

1. Suh, H. *et al. In vivo* fate analysis reveals the multipotent and self-renewal capacities of Sox2$^+$ neural stem cells in the adult hippocampus. *Cell Stem Cell* **1**, 515–528 (2007).
2. Song, H., Stevens, C.F. & Gage, F.H. Astroglia induce neurogenesis from adult neural stem cells. *Nature* **417**, 39–44 (2002).
3. Barkho, B.Z. *et al.* Identification of astrocyte-expressed factors that modulate neural stem/progenitor cell differentiation. *Stem Cells Dev.* **15**, 407–421 (2006).
4. Lie, D.C. *et al.* Wnt signaling regulates adult hippocampal neurogenesis. *Nature* **437**, 1370–1375 (2005).
5. Galceran, J., Miyashita-Lin, E.M., Devaney, E., Rubenstein, J.L. & Grosschedl, R. Hippocampus development and generation of dentate gyrus granule cells is regulated by LEF1. *Development* **127**, 469–482 (2000).
6. Machon, O., van den Bout, C.J., Backman, M., Kemler, R. & Krauss, S. Role of beta-catenin in the developing cortical and hippocampal neuroepithelium. *Neuroscience* **122**, 129–143 (2003).
7. Solberg, N., Machon, O. & Krauss, S. Effect of canonical Wnt inhibition in the neurogenic cortex, hippocampus and premigratory dentate gyrus progenitor pool. *Dev. Dyn.* **237**, 1799–1811 (2008).
8. Wexler, E.M., Geschwind, D.H. & Palmer, T.D. Lithium regulates adult hippocampal progenitor development through canonical Wnt pathway activation. *Mol. Psychiatry* **13**, 285–292 (2008).
9. Clevers, H. Wnt/β-catenin signaling in development and disease. *Cell* **127**, 469–480 (2006).
10. Miyata, T., Maeda, T. & Lee, J.E. NeuroD is required for differentiation of the granule cells in the cerebellum and hippocampus. *Genes Dev.* **13**, 1647–1652 (1999).
11. Liu, M. *et al.* Loss of BETA2/NeuroD leads to malformation of the dentate gyrus and epilepsy. *Proc. Natl. Acad. Sci. USA* **97**, 865–870 (2000).
12. Tozuka, Y., Fukuda, S., Namba, T., Seki, T. & Hisatsune, T. GABAergic excitation promotes neuronal differentiation in adult hippocampal progenitor cells. *Neuron* **47**, 803–815 (2005).
13. Deisseroth, K. *et al.* Excitation-neurogenesis coupling in adult neural stem/progenitor cells. *Neuron* **42**, 535–552 (2004).
14. Hsieh, J., Nakashima, K., Kuwabara, T., Mejia, E. & Gage, F.H. Histone deacetylase inhibition–mediated neuronal differentiation of multipotent adult neural progenitor cells. *Proc. Natl. Acad. Sci. USA* **101**, 16659–16664 (2004).
15. Gao, Z. *et al. Neurod1* is essential for the survival and maturation of adult-born neurons. *Nat. Neurosci.* **12**, 1090–1092 (2009).
16. Nishimoto, M., Fukushima, A., Okuda, A. & Muramatsu, M. The gene for the embryonic stem cell coactivator UTF1 carries a regulatory element which selectively interacts with a complex composed of Oct-3/4 and Sox-2. *Mol. Cell. Biol.* **19**, 5453–5465 (1999).
17. Ferri, A.L. *et al.* Sox2 deficiency causes neurodegeneration and impaired neurogenesis in the adult mouse brain. *Development* **131**, 3805–3819 (2004).
18. Yuan, H., Corbi, N., Basilico, C. & Dailey, L. Developmental-specific activity of the FGF-4 enhancer requires the synergistic action of Sox2 and Oct-3. *Genes Dev.* **9**, 2635–2645 (1995).
19. Collignon, J. *et al.* A comparison of the properties of Sox-3 with Sry and two related genes, Sox-1 and Sox-2. *Development* **122**, 509–520 (1996).
20. Ambrosetti, D.C., Basilico, C. & Dailey, L. Synergistic activation of the fibroblast growth factor 4 enhancer by Sox2 and Oct-3 depends on protein-protein interactions facilitated by a specific spatial arrangement of factor binding sites. *Mol. Cell. Biol.* **17**, 6321–6329 (1997).
21. Avilion, A.A. *et al.* Multipotent cell lineages in early mouse development depend on SOX2 function. *Genes Dev.* **17**, 126–140 (2003).
22. Bylund, M., Andersson, E., Novitch, B.G. & Muhr, J. Vertebrate neurogenesis is counteracted by Sox1–3 activity. *Nat. Neurosci.* **6**, 1162–1168 (2003).
23. Graham, V., Khudyakov, J., Ellis, P. & Pevny, L. SOX2 functions to maintain neural progenitor identity. *Neuron* **39**, 749–765 (2003).
24. Bani-Yaghoub, M. *et al.* Role of Sox2 in the development of the mouse neocortex. *Dev. Biol.* **295**, 52–66 (2006).
25. Muotri, A.R. *et al.* Somatic mosaicism in neuronal precursor cells mediated by L1 retrotransposition. *Nature* **435**, 903–910 (2005).
26. D'Amour, K.A. & Gage, F.H. Genetic and functional differences between multipotent neural and pluripotent embryonic stem cells. *Proc. Natl. Acad. Sci. USA* **100**, 11866–11872 (2003).
27. Gage, F.H. *et al.* Survival and differentiation of adult neuronal progenitor cells transplanted to the adult brain. *Proc. Natl. Acad. Sci. USA* **92**, 11879–11883 (1995).
28. Ma, Q., Kintner, C. & Anderson, D.J. Identification of *neurogenin*, a vertebrate neuronal determination gene. *Cell* **87**, 43–52 (1996).
29. Farah, M.H. *et al.* Generation of neurons by transient expression of neural bHLH proteins in mammalian cells. *Development* **127**, 693–702 (2000).
30. Guillemot, F. Vertebrate bHLH genes and the determination of neuronal fates. *Exp. Cell Res.* **253**, 357–364 (1999).
31. Hsieh, J. & Gage, F.H. Chromatin remodeling in neural development and plasticity. *Curr. Opin. Cell Biol.* **17**, 664–671 (2005).
32. Brault, V. *et al.* Inactivation of the β-catenin gene by Wnt1-Cre–mediated deletion results in dramatic brain malformation and failure of craniofacial development. *Development* **128**, 1253–1264 (2001).
33. Yang, N., Zhang, L., Zhang, Y. & Kazazian, H.H., Jr. An important role for RUNX3 in human LINE-1 transcription and retrotransposition. *Nucleic Acids Res.* **31**, 4929–4940 (2003).
34. Grove, E.A., Tole, S., Limon, J., Yip, L. & Ragsdale, C.W. The hem of the embryonic cerebral cortex is defined by the expression of multiple Wnt genes and is compromised in Gli3-deficient mice. *Development* **125**, 2315–2325 (1998).
35. Lee, S.M., Tole, S., Grove, E. & McMahon, A.P. A local Wnt-3a signal is required for development of the mammalian hippocampus. *Development* **127**, 457–467 (2000).
36. Shimogori, T., VanSant, J., Paik, E. & Grove, E.A. Members of the Wnt, Fz and Frp gene families expressed in postnatal mouse cerebral cortex. *J. Comp. Neurol.* **473**, 496–510 (2004).
37. Gao, X., Arlotta, P., Macklis, J.D. & Chen, J. Conditional knock-out of beta-catenin in postnatal-born dentate gyrus granule neurons results in dendritic malformation. *J. Neurosci.* **27**, 14317–14325 (2007).
38. Jessberger, S. *et al.* Dentate gyrus–specific knockdown of adult neurogenesis impairs spatial and object recognition memory in adult rats. *Learn. Mem.* **16**, 147–154 (2009).
39. van Praag, H., Shubert, T., Zhao, C. & Gage, F.H. Exercise enhances learning and hippocampal neurogenesis in aged mice. *J. Neurosci.* **25**, 8680–8685 (2005).
40. Muotri, A.R., Zhao, C., Marchetto, M.C.N. & Gage, F.H. Environmental influence on L1 retrotransposons in the adult hippocampus. *Hippocampus* (in press).

ONLINE METHODS

Cell culture. Adult hippocampal NSCs were cultured as described[27]. Adult NSCs were cultured with Dulbecco's modified Eagle's medium/F-12 medium (Invitrogen) containing 20 ng mL^{-1} FGF-2 (Wako), 1% N_2 supplement (Invitrogen), 1% antibiotic-antimycotic (Invitrogen), and 2 mM L-glutamine (Wako) in a 5% CO_2 incubator at 37 °C. For neuronal differentiation, cells were cultured in N2 medium (Invitrogen) containing retinoic acid (1 μM, Sigma), forskolin (5 μM, Sigma) and KCl (40 mM, Wako). Dkk1 (500 ng mL^{-1}, R&D Systems), Wnt3a (50 ng mL^{-1}, R&D Systems) and 5 μM TDZD8 (4-benzyl-2-methyl-1,2,4-thiadiazolidine-3,5-dione, Calbiochem) were added to the medium to determine the effects of Wnt signaling. For the adult neurosphere culture from ND1 cKO mice (**Supplementary Fig. 12**), spheres were cultured on uncoated dishes. Lentivirus expressing GFP or Cre-GFP was introduced to the neurospheres. To examine the effect of Wnt signaling on *Neurod1*$^{-/-}$cells (neurospheres), we added Wnt3a ligand (50 ng mL^{-1}) for 2 d after the removal of FGF2 and epidermal growth factor 2.

Construction of plasmids, shRNA and siRNA. Five copies of the Sox/LEF-binding sites were fused upstream to the 200-bp cytomegalovirus (CMV) minimal promoter carrying a TATA box and linked to the *luciferase* gene (Sox/LEF-TATA). Five copies of the DNA binding sequence for Sox2 (Sox-TATA) and five copies of the DNA binding sequence for TCF/LEF (LEF-TATA) were also fused to the minimal promoter-driven luciferase. The mutant construct containing *Neurod1* promoter–driven *luciferase* (NeuroD1 mutant luciferase in **Fig. 2e**) was designed to contain a mutation in the Sox/LEF site to abolish Sox2 and TCF/LEF binding (AAC AAA G sequence was exchanged to GCT AGC G). The Wnt3, DnWnt, Sox2, HDAC1 and β-catenin–expressing lentiviral vectors were constructed using CSC PW, a third-generation, self-inactivating lentiviral vector[41]. Each expression cassette was subcloned at the 3′ end of the CMV promoter on CSC SP PW. The shRNA for the *Ctnnb1* gene was designed to target the sequence GCA ATC AGC TGG CCT GGT TTG, located in the last exon of the rat β-catenin transcript. It was constructed by connecting a shRNA sequence with a terminator under the murine *U6* promoter. This shRNA cassette was subcloned into the TUHSA CS PW lentiviral vector, which contains cassettes of CMV-EGFP, with the ClaI and PmeI restriction sites, and the U6 promoter with the ClaI and HpaI sites. TUHSA CS PW lentiviral vector was derived from the original CSC SP PW plasmid. The knockdown effect of the *Ctnnb1* shRNA was confirmed by western blot analysis using cell lysate from lentivirus-infected, GFP-positive adult hippocampal NSCs (**Supplementary Fig. 2**). The production of lentivirus has been described elsewhere[42]; the viral titers were greater than 1.5×10^4 transducing units ng^{-1}, as determined by the p24 ELISA assay. The murine *Neurod1* promoter was cloned by PCR from genomic DNA and inserted into CSC PW-Luci at the site of the CMV promoter using the restriction enzyme sites for ClaI and BamHI. Sox-TATA, Sox/LEF-TATA and LEF-TATA luciferase reporter plasmids included the binding sequences of the Sox transcription factor (AAC AAT Gtt tAA CAA TGa aaA ACA ATG ttt TAC AAT Gaa aAT ATC AAT G, where capital letters indicate binding sequences and lowercase letters indicate linker sequences), the Sox and LEF transcription factor (AAC AAA Gtt aAA CAA AGt ttA ACA AAG aaa AAC AAA Gta tAA CAA AG), and the LEF transcription factor (AAC AAA aaa AAC AAA ttt AAC AAA aaa AAC AAA ttt AAC AAA). Synthetic siRNAs targeting *Neurog1*, *Neurog2*, *Ctnnb1* and *Neurod1* rat mRNA were purchased from Ambion (Silencer Select siRNA). The siRNA-targeting Sox2 was custom-synthesized by Ambion (custom Select siRNA).

Immunofluorescence studies. Immunofluorescence studies were performed as described[27]. We used mouse monoclonal antibody to beta-tubulin III (TUJ1, 1:500, Promega), antibody to Sox2 (1:300, Chemicon), goat antibody to NeuroD (1:100, Santa Cruz Biotechnology), mouse antibody to nestin (BD Biosciences), guinea pig antibody to GFAP (1:500, Advanced Immunochemical), mouse antibody to NeuN (1:60, clone A10), mouse monoclonal antibody to Wnt3a (1:100, Abcam), goat antibody to Wnt3 (1:100, Everest), mouse monoclonal antibody to S100β (1:200, Abcam), rabbit monoclonal antibody to calretinin (1:100, Abcam), rabbit antibody to Ki67 (1:150, Abcam), rabbit antibody to doublecortin (1:100, Santa Cruz Biotechnology), rabbit antibody to RUNX3 (1:250, Abcam), rat antibody to BrdU (1:250, Abcam) and DAPI (Wako). To examine the proliferative status of NeuroD1-expressing cells (**Fig. 1**), we injected Fisher 344 rats (7–8-week-old rats) with BrdU (100 mg per kg) once a day for 1 week and used the brain sections for BrdU staining analysis. For the immunostaining analysis of AC3 (**Fig. 6**), additional pretreatment of brain sections was conducted[15]. All secondary antibodies were from Jackson ImmunoResearch. Images were analyzed using a Bio-Rad Radiance confocal imaging system or Carl Zeiss LSM confocal imaging system.

qRT-PCR assays. For qRT-PCR assays, total RNA was extracted from cells by Isogen (Nippon Gene). After DNase I treatment (TURBO DNA-free, Ambion), cDNA was synthesized from 1 μg of purified RNA by the SuperScript II First-Strand cDNA synthesis system (Invitrogen), according to the manufacturer's instructions. qRT-PCR was performed with a real-time PCR machine (Bio-Rad). The reported results of the qRT-PCR assays are the averages of two independent RNA preparations. The PCR cycling parameters were 94 °C for 2 min, 40 cycles at 94 °C for 15 s, 60 °C for 20 s and 72 °C for 40 s. Data analysis was performed using the comparative threshold cycle value (C_t) method.

Luciferase assay. Adult NSCs were electroporated with reporter plasmids by a nucleofector device (Amaxa). *Neurod1-luciferase* in a pGL2-luci plasmid (or mutant *Neurod1-luciferase*) and renilla luciferase (R-luc) as an internal control were co-electroporated into adult NSCs. We measured luciferase activity 48 h after electroporation in 50 μL of lysis supernatant with the Dual-Luciferase Reporter Assay System (Promega) according to the manufacturer's protocol. The luminescence signal was quantified with a luminometer (Lumant LB 9501). The ORF2 region and 5′ UTR of human LINE-1.3 were cloned and inserted into CSC PW (the same constructs were used for the EGFP reporter in **Fig. 8**) at the site of the CMV promoter and into the pGL2-luci plasmid.

ChIP and RT-PCR. ChIP was performed using a kit following the manufacturer's protocol (Upstate). Chromatin from cell extracts (input) or immunoprecipitated with specific antibodies was amplified by PCR using primers designed to flank the Sox/LEF-binding site in the rat *Neurod1* promoter and LINE-1. For primary antibodies, we used antibody to HDAC1 (rabbit, Upstate), antibody to acetyl-histone H4 (rabbit, Upstate), antibody to acetyl-histone H3 (rabbit, Upstate), antibody to dimethyl-histone H3 (Lys4, mouse, Upstate), antibody to dimethyl-histone H3 (Lys9, mouse, Upstate), antibody to Sox2 (rabbit, Chemicon) and antibody to β-catenin (rabbit, Cell Signaling). RT-PCR was performed using total RNA extracted from adult hippocampus NSCs. A total of 1 μg RNA was used for first-strand cDNA synthesis with SuperScript II (GibcoBRL). PCR primer sequences are available on request.

Bioinformatics analysis. The genomic sequences for rat (rn3), human (hg17) and mouse (mm5) and the species-specific annotation for known protein coding genes and LINEs (annotated with RepeatMasker) were obtained from the University of California Santa Cruz public genome database (http://genome.ucsc.edu). Candidate binding sites for Sox2 (WWC AAW G) and TCF/LEF (WWC AAA) were identified on either strand of genomic sequence (W for either A or T and N for either A, C, G or T). Promoters were defined as the regions 6,000 bases upstream and 1,000 bases downstream of the annotated transcriptional start sites of protein coding genes. Full-length (at least 6 kb) LINE elements containing TCF/LEF or Sox2 candidate sites located in promoters were retained. We identified 79, 84 and 25 such LINE elements in the human, mouse and rat genomes, respectively (**Supplementary Tables 1–3**).

Retrovirus injection into adult hippocampus. All animal procedures were performed in accordance with protocols approved by the Institutional Animal Care and Use Committee of the National Institute of Advanced Industrial Science and Technology. We used retrovirus expressing a Cre-GFP fusion protein under the control of the *Sox2* promoter[1,26] ($Sox2^{CRE}GFP$). It has been determined that *Sox2* promoter (3.1 kb) on the retrovirus recapitulates endogenous Sox2 expression similarly in CNS[1]. *Rosa26-egfp* mice (Jackson Laboratory), harboring *egfp* and a *loxP*-flanked stop codon, were crossed with $Ctnnb1^{loxP/loxP}$ mice (Jackson Laboratory). The $Ctnnb1^{loxP/loxP}$ allele contains *loxP* sites flanking exons 2–6 and has been shown to be a conditional null allele[32]. Transduction of Cre recombinase under the *Sox2* promoter deleted the

stop codon to activate GFP expression in Sox2-positive cells (control mice). We injected Sox2^{CRE}GFP retrovirus into *Ctnnb1*$^{lox P/lox P}$ mice that were crossed with a *Rosa26-egfp* reporter line and traced GFP-positive cells that had stem cell–specific deletion of *Ctnnb1*$^{lox P/lox P}$ (β-catenin cKO mice). The retrovirus (1.0–1.5 μL) was injected into either control (*Rosa26-egfp*) or *Ctnnb1*$^{lox P/lox P}$; *Rosa26-egfp* mice ($n = 6$ per group). The retrovirus was stereotactically injected into the dentate gyrus of the hippocampus (anterioposterior −2.5 mm, lateral ±2.0 mm and dorsoventral −2.0 to 2.5 mm from Bregma) with a 26-gauge stainless microinjection needle at a rate of 0.5 μl min^{-1}. The needle remained in place for an additional 2 min to facilitate delivery of the virus. Starting 2 weeks after the retrovirus injection, we injected BrdU (100 mg per kg) once a day for 2 weeks. We killed the mice 3 weeks post-surgery and perfused them with 4% paraformaldehyde solution. Brain sections were cut at a thickness of 30 μm with a microtome (ROM-380, Yamato). An immunohistochemical analysis was performed using a confocal microscope.

Lentivirus injection into adult rat hippocampus. Concentrated lentivirus (1.5 μl) was injected stereotactically into the dentate gyrus of the hippocampus (anterioposterior −3.5 mm, lateral ±2.5 mm and dorsoventral −3.5 mm from Bregma) of adult female CD (Sprague-Dawley [SD]) rats (6–8 weeks old, $n = 6$ per group; **Fig. 5**) with a 26-gauge stainless microinjection needle at a rate of 0.5 μl min^{-1}. To assess LINE-1 promoter activity with lentivirus encoding the LINE-1 ORF2 fragment fused to *gfp* (LINE-GFP; **Fig. 8**), we stereotactically injected lentivirus aliquots injected into the dentate gyrus of young adult rats (7–8 weeks old, $n = 6$). The needle remained in place for an additional 2 min to facilitate delivery of the virus. We injected BrdU (100 mg per kg) once a day for 1 week starting 2 weeks after the initial injection of the virus. The rats were killed 3 weeks post-infection and perfused with 4% paraformaldehyde. Brain sections were cut at a thickness of 30 μm with a microtome (ROM-380, Yamato). An immunohistochemical analysis was performed using a confocal microscope.

41. Miyoshi, H., Takahashi, M., Gage, F.H. & Verma, I.M. Stable and efficient gene transfer into the retina using an HIV-based lentiviral vector. *Proc. Natl. Acad. Sci. USA* **94**, 10319–10323 (1997).
42. Pfeifer, A., Brandon, E.P., Kootstra, N., Gage, F.H. & Verma, I.M. Delivery of the Cre recombinase by a self-deleting lentiviral vector: efficient gene targeting *in vivo*. *Proc. Natl. Acad. Sci. USA* **98**, 11450–11455 (2001).